การออกแบบ และการสังเคราะห์สารยับยั้งโปรตีน PDE5 และการประเมินฤทธิ์ทางชีวภาพ

DESIGN, SYNTHESIS AND BIOLOGICAL EVALUATION OF NOVEL PDE5 PROTEIN INHIBITORS

ฐนชล โสมนรินทร์

THANACHON SOMNARIN

วิทยานิพนธ์นี้เป็นส่วนหนึ่งของการศึกษาตามหลักสูตรปริญญาวิศวกรรมศาสตรมหาบัณฑิต

สาขาวิชาวิศวกรรมชีวการแพทย์

คณะวิศวกรรมศาสตร์

สถาบันเทคโนโลยีพระจอมเกล้าเจ้าคุณทหารลาดกระบัง

พ.ศ.2566

KMITL-2023-EN-M-317-026

DESIGN, SYNTHESIS AND BIOLOGICAL EVALUATION OF NOVEL PDE5 PROTEIN INHIBITORS

THANACHON SOMNARIN

A THESIS SUBMITTED IN PARTIAL FULFILLMENT
OF THE REQUIREMENT FOR THE DEGREE OF
MASTER OF ENGINEERING IN BIOMEDICAL ENGINEERING
SCHOOL OF ENGINEERING
KING MONGKUT'S INSTITUTE OF TECHNOLOGY LADKRABANG
2023

KMITL-2023-EN-M-317-026

หัวข้อวิทยานิพนธ์ การออกแบบ และการสังเคราะห์สารยับยั้งโปรตีน PDE5 และการประเมินฤทธิ์ทางชีวภาพ
นักศึกษา นายฐนชล โสมนรินทร์
รหัสประจำตัว 62601084
ปริญญา วิศวกรรมศาสตรมหาบัณฑิต
สาขาวิชา วิศวกรรมชีวการแพทย์
พ.ศ. 2566
อาจารย์ที่ปรึกษาวิทยานิพนธ์ รศ.ดร.แมทธิว พอล กลีสัน
อาจารย์ที่ปรึกษาวิทยานิพนธ์ร่วม ผศ.ดร.กนกทิพย์ บุณยรัตกลิน

บทคัดย่อ

เราได้นำเสนอวิธีการสังเคราะห์ และการตรวจสอบเอกลักษณ์ของสารยับยั้งโปรตีน PDE5 ทั้ง 29 โครงสร้าง ซึ่งถูกออกแบบ และพัฒนามาจากสารยับยั้งที่มีการรายงานในงานวิจัยของเราก่อนหน้านี้ การปรับปรุงโครงสร้างอนุพันธ์ของ 2,4-diaminoquinazoline และ 2,6-diaminopurine เพื่อเพิ่มประสิทธิภาพการยับยั้งต่อโปรตีน PDE5 และการละลาย รูปแบบการจับ (Binding mode) ระหว่างสารยับยั้งกับโปรตีน PDE5 ถูกกำหนดขึ้นโดยใช้วิธีการจำลองสามมิติ และการเปรียบเทียบความคล้ายกันของโครงสร้างกับสารยับยั้งอื่น ๆ รวมถึงการประยุกต์ใช้เทคนิคการจำลองพลวัตเชิงโมเลกุล (Molecular Dynamic Simulation) ซึ่งแต่ละวิธีการดังกล่าวชี้ให้เห็นข้อสรุปของรูปแบบการจับเดียวกัน การปรับปรุงโครงสร้างทางเคมีถูกออกแบบ และสังเคราะห์ขึ้นเพื่อปรับปรุงประสิทธิภาพการยับยั้ง และการละลาย รวมทั้งได้รับยืนยันรูปแบบการจับของโมเลกุล สารประกอบกลุ่มควินาโซลีน (Quinazoline) แสดงช่วงของค่า IC_{50}s ระหว่าง 0.10-9.39 μM ในขณะที่สารประกอบกลุ่มพิวรีน (Purine) แสดงค่า IC_{50}s ระหว่าง 0.29-43.16 μM โดยสารประกอบที่ 25 มีค่า IC_{50}s เท่ากับ 0.15 μM และความสามารถการละลายสูงขึ้นอย่างมากเมื่อเทียบกับสารละลายต้นแบบ (1.77 mg/ml) นอกจากนี้ยังพบว่ารูปแบบการจับที่ทำนายไว้ มีความสอดคล้องกับ SAR ซึ่งได้รับการตรวจสอบความถูกต้องจากการคำนวณทางคอมพิวเตอร์

Thesis	DESIGN, SYNTHESIS AND BIOLOGICAL EVALUATION OF NOVEL PDE5 PROTEIN INHIBITORS
Student	Mr. Thanachon Somnarin
Student ID.	62601084
Degree	Master of Engineering
Program	Biomedical Engineering
Year	2023
Thesis Advisor	Assoc. Prof. Dr. Matthew Paul Gleeson
Thesis co-advisor	Asst. Prof. Dr. Kanokthip Boonyarattanakalin

Abstract

We report the synthesis, and characterization of twenty-nine new inhibitors of PDE5. Structure-based design was employed to modify our previously reported 2,4-diaminoquinazoline series. Modification include scaffold hopping to 2,6-diaminopurine core as well as incorporation of ionizable groups to improve both activity and solubility. The prospective binding mode of the compounds was determined using 3D ligand-based similarity methods to inhibitors of known binding mode, combined with a PDE5 docking and molecular dynamics based-protocol, each of which pointed to the same binding mode. Chemical modifications were then designed to both increase potency and solubility as well as validate the binding mode prediction. Compounds containing a quinazoline core displayed IC_{50}s ranging from 0.10-9.39 μM while those consisting of a purine scaffold ranging from 0.29-43.16 μM. We identified 25 with a PDE5 IC_{50} of 0.15 μM, and much improved solubility (1.77 mg/mL) over the starting lead. Furthermore, it was found that the predicted binding mode was consistent with the observed SAR validating our computationally driven approach.

ACKNOWLEDGMENTS

I would like to acknowledge and thank you all who helped, supported, and funded my thesis at King Mongkut's Institute of Technology Ladkrabang.

Firstly, I express my deepest gratitude to my thesis advisor and mentor Assoc. Assoc. Prof. Dr. Mathew Paul Gleeson of the Department of Biomedical Engineering at King Mongkut's Institute of Technology Ladkrabang. He generously encouraged, guided, and pushed me to make the most of my research experience. Moreover, he went beyond the role of thesis advisor by mentoring me through all the years in graduated school. I would also like to thank Asst. Prof. Dr. Kanokthip Boonyarattanakalin, my co-advisor from College of Nanotechnology, King Mongkut's Institute of Technology Ladkrabang for her having my back during my thesis research

Secondly, I would like to extend my acknowledgement to my fellow students in CMCL group for their friendship, support, and sincere interest towards my study during all these years. I wish to express my thanks for introducing me to the world of pharmaceutical chemistry.

Additionally, this study has received financial support from KMITL (KREF046402). TS would like to acknowledge financial support from the Faculty of Engineering, KMITL (2563-02-01-037). KI would like to acknowledge support from NSRF via the Program Management Unit for Human Resources & Institutional Development, Research and Innovation (B16F640099) and the Center of Excellence for Innovation in Chemistry (PERCH—CIC), Ministry of Higher Education, Science, Research, and Innovation, Thailand

Finally, an honorable mention goes to my family for their love and always encourage me to get through challenging time. I really appreciated their genuine support to complete this project.

Thanachon Somnarin

Table of Contents

page

List of Tables

page

List of schemes

page

List of Figures

page

List of Abbreviations

mL	=	milliliter
mg	=	milligram
µM	=	micro molar
nM	=	nano molar
nm	=	nanometer
ns	=	nanosecond
ppm	=	part per million
RMSD	=	Root Mean Square Deviation
SD	=	Standard deviation
NMR	=	Nuclear Magnetic Resonance
HPLC	=	High Performance Liquid Chromatography
TLC	=	Thin layer chromatography
MS	=	Mass Spectroscopy
PBS	=	Phosphate Buffer Solution
PDB	=	Protein Data Bank
H_2	=	Hydrogen
N_2	=	Nitrogen
Pd/C	=	Palladium on activated carbon
SAR	=	Structure Activity Relationships
TEA	=	Triethylamine
TFA	=	Trifluoroacetic acid
THF	=	Tetrahydrofuran
MeOH	=	Methanol
DIPEA	=	N, N-Diisopropylethylamine
EtOAc	=	Ethylacetate
pTSA	=	para-toluene sulfonic acid
DMSO	=	Dimethyl sulfoxide
MD	=	Molecular Dynamic
DCM	=	Dichloromethane
QM	=	Quantum Mechanic

PDE5	=	Phosphodiesterase type 5
cGMP	=	cyclic Guanosine monophosphate
NO	=	Nitric oxide
PAH	=	Pulmonary Arterial Hypertension
CONF	=	Conformation
HB	=	Hydrogen Bond
%I	=	%Inhibition
IC_{50}	=	half-maximal inhibitory concentration

Chapter 1
Introduction

1.1 Statement and significance of the problems

The foundation for engineering includes Mathematics, Physics and Chemistry. Biomedical Engineering is very diverse in its applications. Traditionally, it has been focused on Instrumentation (electronics) and Mechanical (physics) but recently, it can really involve anything related to human use product technology or even medical chemistry. Drug design refers to everything associated with the development of a drug in connection with chemistry, from the initial design to the final delivery of the drug. Thus, it covers a very broad area of ground rational design of the drug by molecular modeling base on basic principle of computational, physical and organic chemistry, followed by the synthesis of a very great many chemical products and must be characterized in a many process to produce a hit.[1] A huge number of hit molecules are going to be tested with the specific target and studied in the pharmacokinetics within an organism. The parameters ADME (Absorption, Distribution, Metabolism and Excretion) are examined so that the chemist can modify the compounds to improve on these various points. After that, the hit molecule will be selected to lead and put into the human clinical trial process to further identify to candidate drug.

Pulmonary arterial hypertension (PAH) is a debilitating cardiovascular disease suffered by 15 out of every million people.[2] The disease involves extensive remodeling and narrowing of the blood vessels, resulting in an increased workload for the right ventricle of the heart, leading to its eventual failure and patient death.[3, 4] The majority of patients suffering from PAH (~54%) are treated with phosphodiesterase 5 (PDE5) inhibitor monotherapy.[5] PDE5 is an important enzyme on the cyclic guanosine monophosphate (cGMP) / nitric oxide signaling pathway. PDE5 inhibitors can produce acute vasodilatory effects through inhibition of cGMP. Inhibition of the target can reduce the vasodilation effect of cGMP. The cGMP accumulation augments the nitric oxide (NO) induced vascular smooth muscle relaxation.[6] Unfortunately, current PDE5 drugs, including Sildenafil and Tadalafil (Figure 3), result
in adverse effects including nasal congestion, diarrhea, vomiting, fever, skin disorders, pain in limbs and visual abnormalities.[7-9]

Many PDE5 inhibitors employ bicyclic scaffolds due to their ability to form **π**-stacking interactions with residues such as Phe-820 and Phe786 which help define the top and bottom of the active site, respectively, along with residues Tyr762, Leu765 and Val782. These interactions help orientate the molecule towards H-bonding with Gln817 to the residue within the active site. Analysis of 38 X-ray structures reported in the protein databank[10] show that 86% make directly H-bond interactions with Gln817, and of these 75% make a bi-dentate interaction

The quinazoline scaffold has been used in a variety of different PDE5 chemistry studies, including the 4-subsituted variants of Watanabe[11], the 2 & 4-substituted variants of Lee et al,[12] and Pobsuk et al[13] and related variants such as the 1,3 aminopyrazinone of Hughes et al.[14] In our previous work, we reported compound **A**[13, 15] a potent PDE5 inhibitor with sub μM activity. *Ex-vivo* assessment in a rat pulmonary artery vasodilation model demonstrated the compounds were only 10-fold less active than the drug Sildenafil. The *ex vivo* IC_{50} of 1.63 ± 0.72 μM compared to 0.14 for Sildenafil. However, the compound had relatively low phosphate buffer solubility at 0.56 mg/mL and a moderately high predicted clogP was 3.9.

In this follow-up study we have applied computational approaches to determine the most probable binding mode of the series to PDE5. This was performed to facilitate the structure-based design of new, more potent, and soluble derivatives. A consensus modeling approach to determining the binding mode was performed; structure-based design methods to evaluate a range of different potential poses (molecular docking, quantum mechanical (QM) optimization and molecular dynamics) and ligand-based-design methods (shape and pharmacophore) to determine the 3D overlap of the chemotype to drugs with confirmed X-ray-derived binding modes (Figure 1).

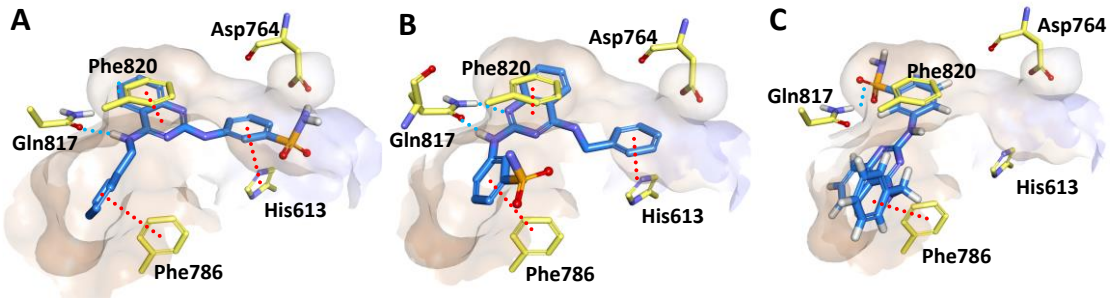

Figure 1. Docking of **A** to PDE5 led to 3 distinct binding mode to PDE5. A molecular-dynamics simulation was subsequently used to determine which represented the most stable protein-ligand complex.

The consensus computational approach led to the identification of a single binding mode consistent with experimental observations. Synthetic modifications to the chemotype were subsequently developed, focusing on the scaffold itself and steric and electronic modification to groups at the 2 & 4 positions. Modifications were designed to; (a) validate the proposed binding mode from computational modelling (b) increase the binding affinity of the molecule by improving H-bonding and **π**-stacking interactions with active site residues and (c) incorporation of more polar and/or ionizable groups, in positions where they are tolerated, to increase solubility. (Figure 2)

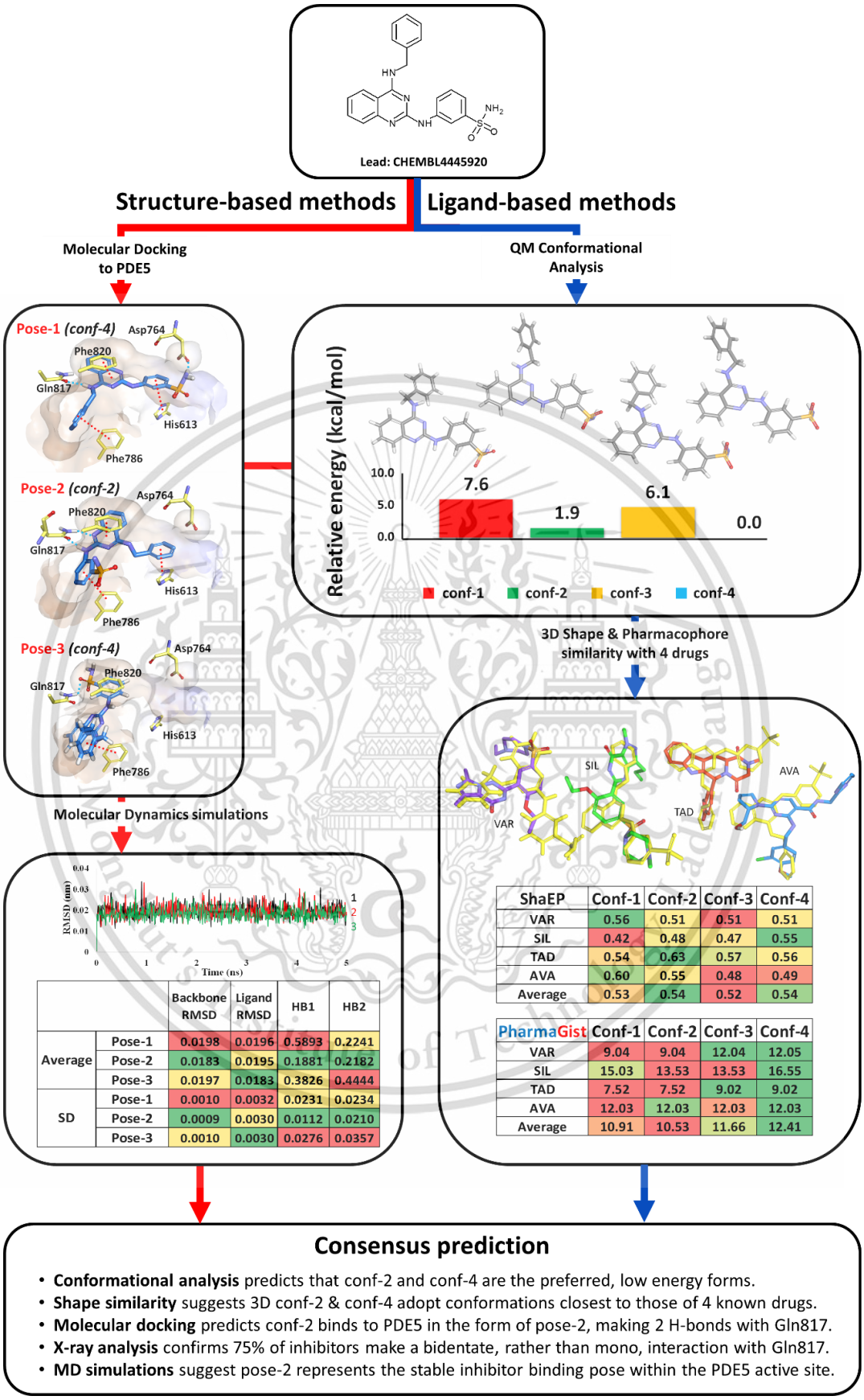

		Backbone RMSD	Ligand RMSD	HB1	HB2
Average	Pose-1	0.0198	0.0196	0.5893	0.2241
	Pose-2	0.0183	0.0195	0.1881	0.2182
	Pose-3	0.0197	0.0183	0.3826	0.4444
SD	Pose-1	0.0010	0.0032	0.0231	0.0234
	Pose-2	0.0009	0.0030	0.0112	0.0210
	Pose-3	0.0010	0.0030	0.0276	0.0357

ShaEP	Conf-1	Conf-2	Conf-3	Conf-4
VAR	0.56	0.51	0.51	0.51
SIL	0.42	0.48	0.47	0.55
TAD	0.54	0.63	0.57	0.56
AVA	0.60	0.55	0.48	0.49
Average	0.53	0.54	0.52	0.54

PharmaGist	Conf-1	Conf-2	Conf-3	Conf-4
VAR	9.04	9.04	12.04	12.05
SIL	15.03	13.53	13.53	16.55
TAD	7.52	7.52	9.02	9.02
AVA	12.03	12.03	12.03	12.03
Average	10.91	10.53	11.66	12.41

Figure 2. Flow chart, shows the methods used to identify of the putative binding mode of A to PDE5.

1.2 Goal and Objective

We are going to merge features of PDE5 inhibitor and known PDE5 drug Sildenafil[16], especial ring, hydrophobic region modification and apply basic center in order to tightly bind in active site of protein target and solubility improvement, then synthesized the series of 20 compounds and assessed within biochemical and biological assays by our established academic collaborators.

1. To get better understanding about Structure Activity Relation (SAR) and design PDE5 inhibitors using structure-base and ligand-base method

2. To Synthesize 20 novel compounds based on 2,4-diaminoquinazoline and 2,6-diaminopurine scaffold as inhibitors to potent PDE5 protein.

3. To discover the new route of synthesis to make the compounds associated with PDE5 inhibitor.

4. To evaluate biological activity, selectivity, potency of PDE5 inhibitors that we have synthesized, assay toxicity and solubility of compounds and publish the new knowledge.

1.3 Scope of the study

This research emphasizes the development of methods for Pulmonary arterial hypertension treatment in drug form. The research involves a multi-disciplinary study effort covering. (a) computational inhibitors target analysis, (b) 2,4-diaminoquinazoline and 2,6-diaminopurine based compounds synthesis and characterization and (c) biological assay being performed by established our collaborator in Thailand.

Chapter 2

Theory and Literature Reviews

2.1 Pulmonary Arterial Hypertension (PAH) disease

Pulmonary hypertension is defined as a resting mean pulmonary artery pressure of 25 mm Hg or above. Pulmonary arterial hypertension (PAH), a type of pulmonary hypertension that primarily affects the pulmonary vasculature. PAH is a disease of the cardiopulmonary unit, affecting the pulmonary arterial and venous circulation and the right ventricle. Obstructive, hyperproliferative, vascular lesions, blood vessel constriction of pre-capillary arterioles, and pulmonary vascular resistance (PVR) is increased by venous obstruction, then increase right ventricular afterload, and stimulate right ventricular failure (RVF), which is leading to cause of death in PAH if left untreat.[17, 18]

The incidence of PAH ranges from 2.0 to 7.6 cases per million adults per year, and its prevalence varies from 11 to 26 cases per million adults. The incidence of PAH is 4-fold higher in women than in men. In contrast, survival is worse in men with PAH.[19] In the longitudinal observational study of population in United Kingdom and Ireland between 2001-2009 shown that, the incidence of PAH of 1.1 cases per million per year and prevalence of 6.6 cases per million.[20] The data from Asia, 148 of patients were diagnosed, The most common aetiologies were congenital heart disease associated PAH (35.8%), idiopathic PAH (29.7%) and then connective tissue disease-associated PAH (24.3%). More importantly, the most of patients about 54.1% were on phosphodiesterase type 5 (PDE5) inhibitor monotherapy.[5]

2.2 PAH and ED drugs on market

Prostacyclin analogues act on the prostacyclin pathway to enhance cAMP level and augment vasodilation, inhibiting both platelet aggregation and smooth muscle cell proliferation. Injectable agents include epoprostenol and treprostinil, administered by continuous IV infusion because they are kind of short half-lives. Additionally, treprostinil is available for subcutaneous infusion, as well as both inhaled and oral routes.[21]

Sildenafil, the PDE5 inhibitor, was selected as candidate drug for clinical development in 1989. Over a decade, it was approved by the US Food and Drug

Administration (USFDA) for use in erectile dysfunction treatment. In 2005, sildenafil was published for use to treat PAH in adults. However, there are many side effects in sildenafil such as cough and nasal congestion, diarrhea and vomiting, fever, skin disorders, pain in limbs and visual abnormal.[7, 16]

Tadalafil is a selective PDE5 inhibitor and was approved for treatment of erectile dysfunction in the US, and for PAH in 2011. Tadalafil have been using in a tablet of 20 mg for cure pulmonary hypertension under the brand name Adcirca. Like sildenafil, it was tolerated with mild to moderate adverse events.[22]

Ambrisentan is the once daily oral medication for PAH therapy, using in endothelin pathway. It has an indication for use combinatory therapy with tadalafil for Group 1 of PAH. For the treatment of PAH to improve exercise capacity, hemodynamic, delay disease progression and reduce hospitalizations.[23]

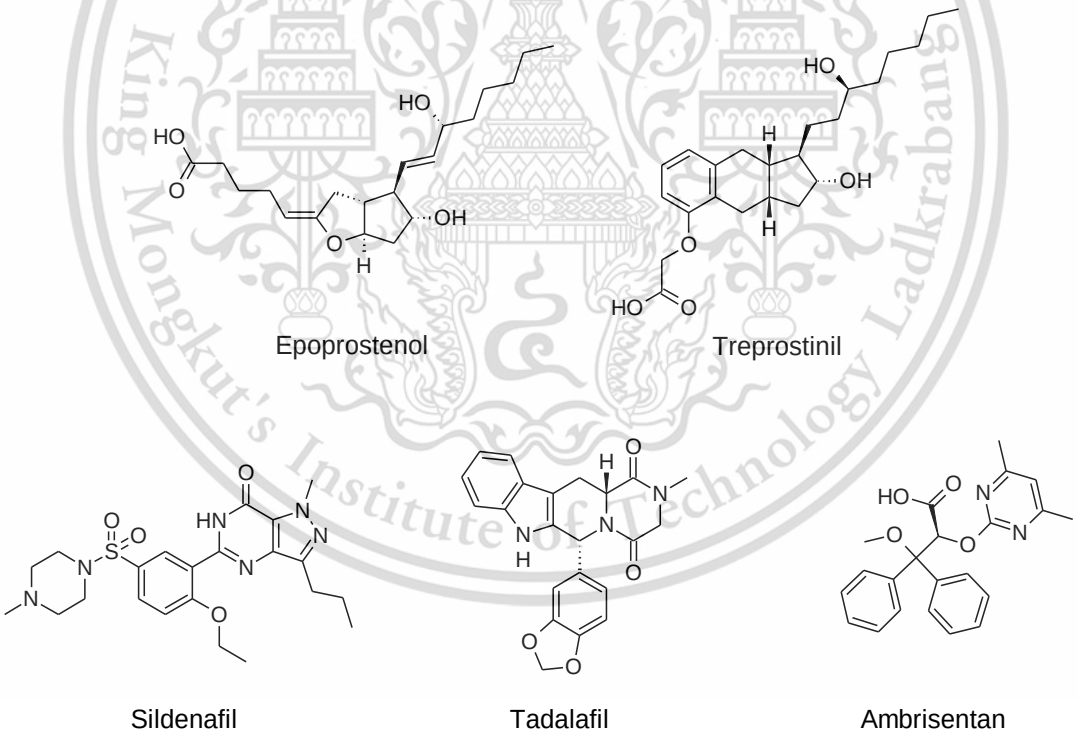

Figure 3 The structure and name of known drugs for treatment of PAH on the market.

2.3 Targets of interest in this study

The pathobiology of Pulmonary hypertension related with vasoconstriction (meaning reduction of products in vasodilation pathway such as prostacyclin and nitric oxide), endothelial dysfunction, smooth muscle cell proliferation and thrombosis. Signaling pathways involved in these processes are important targets for treatment of PAH.[24] The nitric oxide signaling pathway is an interested target, nitric oxide is synthesized in pulmonary vascular endothelial cell and move inside smooth muscle cell then activate the guanylyl cyclase enzyme. cGMP is converted by the enzyme and GTP which can decrease the calcium ion influx, resulting in the vascular smooth muscle relax.[25] cGMP degradation is occurred by binding with PDE5 protein on the catalytic domain. This active site consists of the key binding residues such as Q817, H613 (Glutamine817 and Histidine613 respectively) which position the cyclic phosphate group toward the magnesium and zinc ions where near the H613 and bound water molecules in the site and align amide to bind with Q817, these interactions are involved in the hydrolysis step. The several approved PDE5 inhibitors, for instance sildenafil or Vardenafil are similar to cGMP structure, because they have purinone-like cores. Therefore, can replace the cGMP on catalytic site leading to blocking the cGMP hydrolysis process and increase the level of cGMP, vasodilation, resulting in good blood circulation.[26]

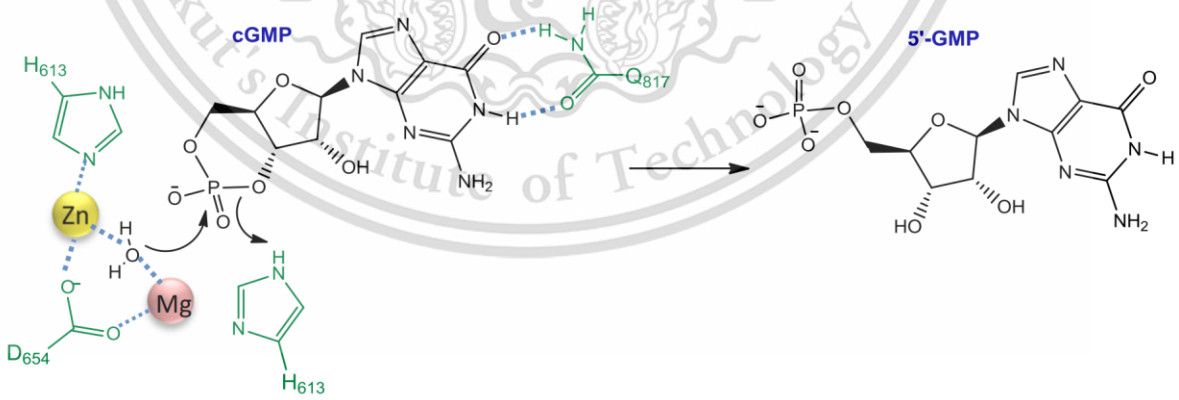

Figure 4 The general mechanism of cGMP hydrolysis on PDEs catalytic site and shown the associate residue interactions.[26]

2.4 Phosphodiesterase 5 (PDE5) and cGMP

PDE5 is a multidomain protein and can be split into a regulatory part and a catalytic domain. The regulatory part is located at the N-terminal side, consists of two GAF (GAFa & GAFb) domains in tandem which are involved in controlling the catalytic activity as well as dimerization of the protein and the catalytic domain is located at the C-terminal of protein.[27] GAFa is the cGMP-binding domain that mediates allosteric regulation of PDE5 activity.[28] PDE5 is one of the most well-studied phosphodiesterases (PDEs) that specifically targets cGMP typically generated by nitric oxide (NO)-mediated activation of the soluble guanylyl cyclase. In the endothelial cell cytoplasm, NO is generated from L-arginine by the control of endothelial nitric oxide synthases (eNOS), NO will be released out of endothelial cell directly into the smooth muscle cells and form with guanylyl cyclase resulting in convert the guanosine 5'-triphosphate (GTP) into 3'-5'-cyclic guanosine monophosphate (cGMP). After that, cyclic GMP is interacted with protein kinase (PKG). These interactions cause to reduce calcium ion influx resulting in the relaxation of arterial and smooth muscle leading to arterial dilatation (Vasodilation). cGMP can be degraded by hydrolysis of PDE5 protein, the degradation happens in the catalytic domain, it will be bound within PDE5 active site with hydrogen bonds and consequently decrease the cGMP level leading to contraction of smooth muscle.[29]

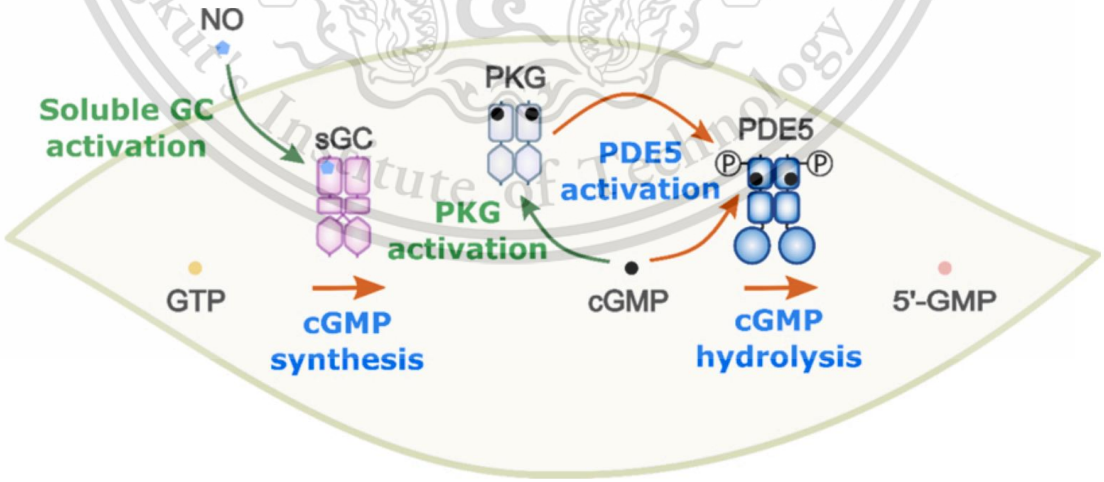

Figure 5 The bio-signaling of action of PDE5 and cGMP pathway in smooth muscle cells.[30]

2.5 Quinazoline and Purine like cores

Among heterocyclic compounds, the quinazoline template seems to be mostly interested by several researchers. Contributing factors for their desirability include: (a) facile synthetic access, (b) lead-like and drug-like attributes and (c) high opportunities that the quinazoline can be active in molecule target led to development of lead optimizations. For instance, quinazoline derivative for cancer treatment such as lapatinib and gefitinib.[31, 32] In addition, 2, 4-diaminoquinazoline also has been synthesized for against *Leishmania donovani* which cause to debilitating disease.[33] In the recent past, purine based molecules have emerged as significantly potent the several target, particularly kinase inhibitors.[34] 2,9-disubstituted 8-phenylthio/phenylsulfinyl-9H-purine scaffold was investigated and some of their series were synthesized to inhibit the EGFR kinase with high potential (IC_{50} = 1.9 nM),[35] in case antitumor agents,[36] or in the treating of acute leukemias (thiopurines).[37]

2.6 Structure-based design

The first method of drug discovery process is to design the ligand that can selectively bind to specific enzyme like the fitting of lock and key which including two main processes. SAR study is the indirect process to find and make up the novel series of inhibitors via integration of structure activity relationship (SAR) for compounds derived from chemical properties improvement and given a measurable biological or therapeutic activity without having any details of image of enzyme target. Structure base-design is the more direct method using tree-dimensional (3D) structure of ligand and target to design the new inhibitors which must have known the detail of each site of enzyme target before attempting to create the ligands in order to confirm to be specific for the target.[38] Structure base-design can also help to significantly reduced times and cost associated with drug discovery process.

Compounds have undergone using 3D structure overlays from the related protein structure templates taken from the Protein data bank (PDB). this report has generated crystal structure of Sildenafil as the PDE5 inhibitor within active site of PDE5 protein (PDB code: 1UDT).[39] The Characteristic binding and Interaction between Sildenafil with each residue in PDE5 active site have presented in the PDE5 docking (**Figure 6**). This helps us

to confirm how the known inhibitor interacted with the key amino acids in active site of this protein.

Additionally, our previous work has reported a series of N^2, N^4-diaminoquinazoline as the PDE5 inhibitors, the computation docking was used to facilitate the observed interaction. The PDE5 pocket site is shown as a surface bubble with amino acid residues (yellow). CHEMBL4445920, the blue structure was put in the catalytic site, it made one H-bond interaction between -C=O group of Gln817 via NH-atom as H-bond donor at the 4-position of ligand and formed the required **π**-stacking interaction with Phe820 and Phe786, NH_2- on sulfonamide group also forms H-bond interaction through -C=O group of Asp764. This compound exhibited high potency to inhibit PDE5 protein with IC_{50} 0.010 **μ**M and shown 4.6-folds selectivity over PDE6.[40] (**Figure 6**)

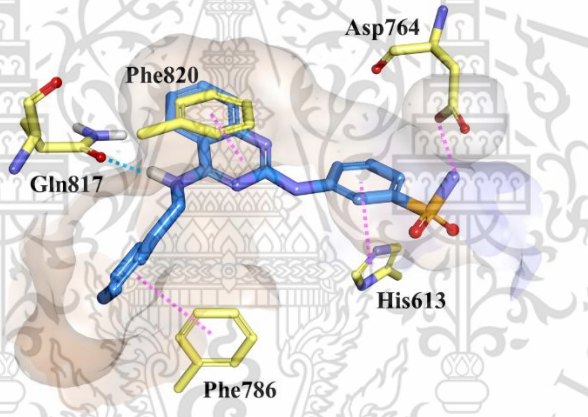

Figure 6. The predicted binding mode of our previous work show the interaction between ligand and the amino acid residues in the PDE5 active site.

Chapter 3

Material and Method

3.1 Material

3.1.1 Instruments

^{1}H NMR spectra and ^{13}C NMR were recorded on a NMR 500 MHz (Brand: Jeol, spectrometer model: ECZ500/S1). The Chemical shifts were reported in part per million (ppm) using TMS as the residual solvent line as the internal standard. ^{1}H NMR and ^{13}C NMR use DMSO-d^{6} as the solvent for measurement the peaks, the solvent peak and water peak are 2.5 ppm and 3.5 ppm. respectively.

The coupling constant (*J*) are reported in Hz, and the patterns are designed as singlet (s), doublet (d), doublet of doublet (dd), triplet (t), quartet (q) and multiplet (m), meaning is the measure of the interaction between a pair of protons.

High Performance Liquid Column Chromatography (HPLC) was used for measured >95% purity based on a UV absorbance HPLC chromatogram (Agilent 1100 system and HITACHI/Chromaster, Sunshell C8 column using a mobile phase consisting of (a) 0.1% formic acid in water and (b) acetonitrile: 99:1% to 1:99% gradient run in 7 minutes)

Mass spectra (MS) were performed on AGILENT 1100 HPLC instrument coupled to a LC|MSD Trap mass spectrometer, in ESI (+) mode or APCI mode or using a High-Resolution Mass Spectrometry (HRMS) were measured on Bruker micrOTOF-Q III in ESI (+) mode at Faculty of Science, Kasetsart University.

3.1.2 Column and Thin Layer Chromatography

Thin Layer Chromatography (TLC) was used to monitor for all of reactions, was conducted on aluminum/silica gel plate. The chromatograms were visualized under UV light 254 nm. Utilizing different solvent systems, depending on the polarity of each compound. In this research methanol in dichloromethane and ethyl acetate in dichloromethane were used mostly.

Column chromatography was performed using SiO_2 (particle size 0.040–0.055 mm, 230–400 mesh, is the method for purify all compound in these series. The silica gel was used to pack the column, eluting by different solvent system. Mostly, 75%DCM/25%EtOAc and 98%DCM/2%MeOH were used in these series.

3.1.3 Chemical reagents

The reagents, building blocks and solvents obtained from commercial suppliers were used without further purification.

3.2 Computational Method

3.2.1 Quantum Chemical Calculations

Four different conformations of **A** were generated in Discovery studio by rotating the relative orientation of groups at the 2-position and 4-position of quinazoline to either 0 or 180 degrees. Quantum mechanical geometry optimization (HF/6-31G(d)) was performed in Gaussian G16[41] using default settings.

3.2.2 Ligand-based Similarity Methods

The shape-based and pharmacophore-based overlap between the 4 optimized conformation of **A** and PDE5 reference inhibitor conformations extracted from experimental PDB structure were undertaken. The active conformations of Vardenafil (1XP0[42]), Sildenafil (1UDT[43]), Tadalafil (1XOZ[42]), and Avanafil (6L6E[44]) were extracted from the PDB structure and used as references. Shape-based overlap to Sildenafil, Tadalafil, Avanafil and Vardenafil were performed using both volume-based and charge-based overlap option in ShaEP.[45] The pharmacophore-based overlap was performed using PharmaGist.[46, 47] Program defaults were used and the overlap score of each pair was evaluated, a higher score indicates better overlapping. This score could then be used to infer the most probable binding mode.

3.2.3 Molecular Docking

Molecular docking of **A** to the PDE5 protein conformation adopted in co-complexes with Vardenafil (1XP0[42]), Sildenafil (1UDT[43]), Tadalafil (1XOZ[42]), and Avanafil (6L6E[44]) were undertaken. All co-factors, ligands and water molecules were removed from the protein and docking with GOLD5.3 was undertaken.[48] Default setting were apart from the imposition of a H-bond constraint between the ligand and Gln817. This led to the identification of 3 distinct binding poses being generated in the different PDE5 protein conformations.

3.2.4 Molecular Dynamics (MD) Simulations

MD simulations were performed on the 3 binding poses of **A** docked to 1XP0.[42] Simulations were carried out using the program GROMACS v. 2019.4[49] in conjunction with the AMBER99SB forcefield.[50, 51] The restrained electrostatic potential (RESP) charge

of the ligand was determined from a Hartree-Fock calculation with the 6-31G(d) basis set. Ligands topology files were created using the ACPYPE script[52] with the GAFF forcefield.[53, 54] The protonation state of amino acid residues were confirmed based on their predicted pK_a calculated using Propka3.1[55, 56] and a visual assessment of the local interactions. The protein was immersed in a box of TIP3P water molecules with a minimum distance of 12 Å between the protein and box edge.[57] NaCl ions were added (0.15 M). The system was minimized to an RMS gradient of 10 kJ mol^{-1} nm^{-1} to relax any steric conflicts. The system was heated from 0 to 300 K over 500 ps using an NVT scheme followed by equilibration for 1 ps. The system underwent production dynamics using an NPT ensemble for 5 ns. Simulations used the Parrinello-Rahman barostat,[58] a 2 fs time step and particle mesh Ewald.[59] All bonds were constrained using LINCS algorithm.[60]

3.3 Synthesis

Twenty-nine novel compounds were synthesized in total according to **Scheme 1** with overall reaction yields ranging from low (~3.0%), for 9*H*-purines, to excellent (~80%), for quinazolines lacking a basic center.

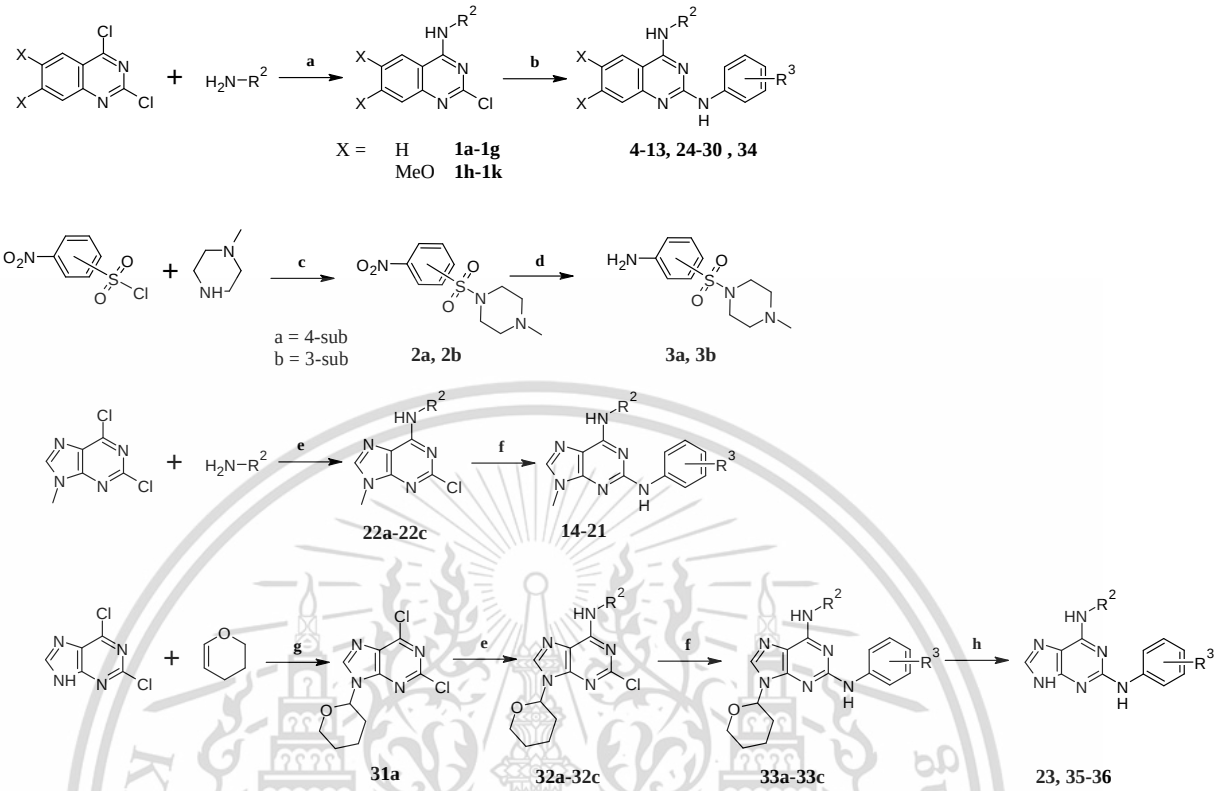

Scheme 1. General synthesis of PDE5 inhibitors; (a) TEA, THF at room temperature for 6-8 hrs, (41.9-99.1%), (b) 1M HCl, IPA at 90°C for 8 hrs, (8.1-92.5%), (c) TEA 0.5 mL in DCM, 0 °C - rt for 2 hrs, (82.6-91.8%), (d) H_2, Pd/C in MeOH at rt for 2 hrs, (67.8-95.5%) (e) R^2-NH_2, DIPEA, n-butanol at 90°C for 6 hrs, (27.2-85.4%), (f) R^3-NH_2, $Pd_2(dba)_3$, Xphos, K_2CO_3, 1,4-dioxane anhydrous at 110°C overnight, (25.1-72.0%), (g) pTSA in EtOAc at rt for 5 hrs, (h) TFA in DCM at rt, 3-5 hrs,, (14.9-78.4%).

3.3.1 General synthesis procedure A

A mixture of 2,4-dichloroquinazoline (1.0 eq) and amine (1.2 eq) was stirred for 10 min in THF (20 ml), TEA (0.50 ml) was added in a solution, keep stirred the reaction at ambient temperature for 6-8 h until its completion. The resulting mixture was evaporated, washed with 40 ml. saturated NaCl in water and extracted with ethyl acetate (3 x 20 ml). the organic layers were combined, dried over anhydrous Na_2SO_4. Finally, the residue was further purified by silica gel column chromatography with DCM/EtOAc = 3/1

3.3.1.1 2-chloro-N-[(thiophen-2-yl) methyl] quinazolin-4-amine (1a)

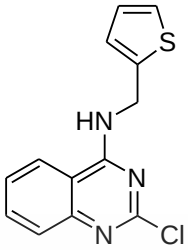

2,4-dichloroquinazoline (1.0 eq, 2.51 mmol) and 1-(thiophen-2-yl) methanamine (1.2 eq, 3.01 mmol), following the general synthetic procedure A to give the desired compound 1a as a white solid with 71.36% yield. ^{1}H-NMR (500 MHz, DMSO-d^{6}) δ 11.31 (s, 1H), 8.58 (d, *J* = 7.9 Hz, 1H), 7.83 – 7.74 (m, 1H), 7.51 (dd, *J* = 5.1, 1.3 Hz, 1H), 7.36 – 7.30 (m, 2H), 7.25 (dd, *J* = 3.4, 1.0 Hz, 1H), 7.02 (dd, *J* = 5.1, 3.5 Hz, 1H), 5.09 (d, *J* = 3.6 Hz, 2H). MS-ESI: m/z 276.1 [M+H]+.

3.3.1.2 2-chloro-N-benzyl-2-chloroquinazolin-4-amine (1b)

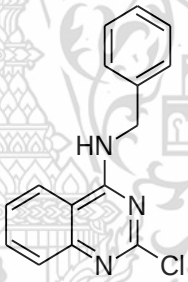

2,4-dichloroquinazoline (1.0 eq, 2.51 mmol) and benzyl amine (1.2 eq, 3.01 mmol), following the general synthetic procedure A to give the desired compound 1b as a white solid with 52.73% yield. ^{1}H-NMR (500 MHz, DMSO-d^{6}) δ 9.26 (t, *J* = 4.6 Hz, 1H), 8.28 (dd, *J* = 6.6, 0.5 Hz, 1H), 7.77 (t, *J* = 6.1 Hz, 1H), 7.60 (d, *J* = 6.6 Hz, 1H), 7.51 (t, *J* = 5.7 Hz, 1H), 7.32 (dt, *J* = 12.1, 5.9 Hz, 4H), 7.22 (t, *J* = 5.7 Hz, 1H), 4.72 (d, *J* = 4.7 Hz, 2H). MS-ESI: m/z 270.0 [M+H]+.

3.3.1.3 2-chloro-N-propylquinazolin-4-amine (1c)

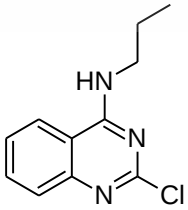

2,4-dichloroquinazoline (1.0 eq, 2.51 mmol) and propyl amine (1.2 eq, 3.01 mmol), following the general synthetic procedure A to give the desired compound 1c as a white solid with 60.64% yield. ^{1}H-NMR (500 MHz, DMSO-d^6) δ 8.68 (t, *J* = 4.1 Hz, 1H), 8.23 (dd, *J* = 6.6, 0.6 Hz, 1H), 7.74 (ddd, *J* = 6.7, 5.6, 1.0 Hz, 1H), 7.56 (dd, *J* = 6.7, 0.5 Hz, 1H), 7.48 (ddd, *J* = 6.5, 5.6, 0.9 Hz, 1H), 3.43 (dd, *J* = 10.2, 5.7 Hz, 2H), 1.62 (dd, *J* = 11.6, 5.9 Hz, 2H), 0.90 (t, *J* = 5.9 Hz, 3H). MS-ESI: m/z 222.1 [M+H]+.

3.3.1.4 2-chloro-N-(2-methylpropyl) quinazolin-4-amine (1d)

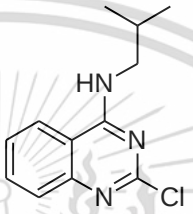

2,4-dichloroquinazoline (1.0 eq, 2.51 mmol) and isobutyl amine (1.2 eq, 3.01 mmol), following the general synthetic procedure A to give the desired compound 1d as a white solid with 41.94% yield. ^{1}H-NMR (500 MHz, DMSO-d^6) δ 8.69 (s, 1H), 8.26 (d, *J* = 6.1 Hz, 1H), 7.75 (t, *J* = 5.6 Hz, 1H), 7.57 (d, *J* = 6.6 Hz, 1H), 7.49 (t, *J* = 5.7 Hz, 1H), 3.29 (d, *J* = 4.7 Hz, 2H), 2.00 (dt, *J* = 10.9, 5.4 Hz, 1H), 0.90 (s, 3H), 0.89 (s, 3H). MS-ESI: m/z 236.1 [M+H]+.

3.3.1.5 2-chloro-N-[1-(propan-2-yl) piperidin-4-yl] quinazolin-4-amine (1e)

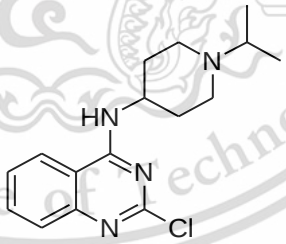

2,4-dichloroquinazoline (1.0 eq, 2.51 mmol) and 1-(propan-2-yl) piperidin-4-amine (1.2 eq, 3.01 mmol), following the general synthetic procedure A to give the desired compound 1e as a yellow solid with 58.4% yield. ^{1}H-NMR (500 MHz, DMSO-d^6) δ 8.35 (d, *J* = 6.1 Hz, 1H), 8.31 (d, *J* = 6.6 Hz, 1H), 7.74 (t, *J* = 5.6 Hz, 1H), 7.56 (d, *J* = 6.0 Hz, 1H), 7.48 (t, *J* = 5.6 Hz, 1H), 4.07 – 3.99 (m, 1H), 2.80 (d, *J* = 9.4 Hz, 2H), 2.69 (dt, *J* = 10.5, 5.2 Hz, 1H), 2.19 (t, *J* = 8.8 Hz, 2H), 1.86 (d, *J* = 7.6 Hz, 2H), 1.59 (dd, *J* = 16.1, 9.5 Hz, 2H), 0.95 (s, 3H), 0.93 (s, 3H). MS-ESI: m/z 305.1 [M+H]+.

3.3.1.6 N2-(2-chloroquinazolin-4-yl)-N1, N1-dimethylethane-1,2-diamine (1f)

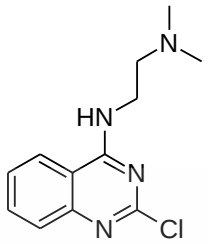

2,4-dichloroquinazoline (1.0 eq, 2.51 mmol) and N^1,N^1-dimethylethane-1,2-diamine (1.2 eq, 3.01 mmol), following the general synthetic procedure A to give the desired compound 1f as a yellow solid with 67.9% yield. ^{1}H-NMR (500 MHz, DMSO-d^6) δ 8.69 (s, 1H), 8.25 (d, *J* = 7.5 Hz, 1H), 7.79 (t, *J* = 7.0 Hz, 1H), 7.62 (d, *J* = 7.6 Hz, 1H), 7.53 (t, *J* = 7.0 Hz, 1H), 3.62 (d, *J* = 5.4 Hz, 2H), 2.54 (d, *J* = 6.6 Hz, 2H), 2.21 (s, 6H). MS-ESI: m/z 251.1 [M+H]+.

3.3.1.7 N-(1-benzylpiperidin-4-yl)-2-chloroquinazolin-4-amine (1g)

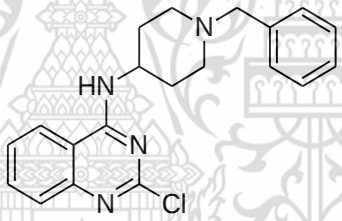

2,4-dichloroquinazoline (1.0 eq, 2.51 mmol) and 1-benzylpiperidin-4-amine (1.2 eq, 3.01 mmol), following the general synthetic procedure A to give the desired compound 1g as a brown solid with 66.11% yield. ^{1}H-NMR (500 MHz, DMSO-d^6) δ 8.40 (d, *J* = 6.5 Hz, 1H), 7.75 (t, *J* = 6.6 Hz, 1H), 7.57 (d, *J* = 6.3 Hz, 1H), 7.48 (t, *J* = 5.4 Hz, 2H), 7.36 (s, 3H), 7.30 (d, *J* = 4.2 Hz, 2H), 4.20 (s, 1H), 3.01 (d, *J* = 5.9 Hz, 4H), 1.95 (s, 4H). MS-ESI: m/z 353.2 [M+H]+.

3.3.1.8 2-chloro-6,7-dimethoxy-N-propylquinazolin-4-amine (1h)

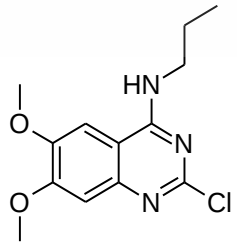

2,4-dichloro-6,7-dimethoxyquinazoline (1.0 eq, 1.93 mmol) and propyl amine (1.2 eq, 2.32 mmol), following the general synthetic procedure A to give the desired compound 1h as a white solid with 78.16% yield. ^{1}H-NMR (500 MHz, DMSO-d^6) δ 8.30 (t, *J* = 4.3 Hz, 1H), 7.58 (s, 1H), 7.02 (s, 1H), 3.84 (s, 6H), 3.40 (t, *J* = 4.6 Hz, 2H), 1.61 (dd, *J* = 11.6, 5.9 Hz, 2H), 0.90 (t, *J* = 5.9 Hz, 3H). MS-ESI: m/z 282.0 [M+H]+.

3.3.1.9 2-chloro-6,7-dimethoxy-N-isopropylquinazolin-4-amine (1i)

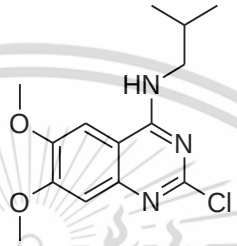

2,4-dichloro-6,7-dimethoxyquinazoline (1.0 eq, 1.93 mmol) and isobutyl amine (1.2 eq, 2.32 mmol), following the general synthetic procedure A to give the desired compound 1i as a white solid with 67.63% yield. ^{1}H-NMR (500 MHz, DMSO-d^6) δ 8.30 (t, *J* = 4.4 Hz, 1H), 7.61 (s, 1H), 7.02 (s, 1H), 3.84 (s, 3H), 3.84 (s, 3H), 3.27 (s, 2H), 2.01 – 1.94 (m, 1H), 0.91 (s, 3H), 0.89 (s, 3H). MS-ESI: m/z 296.1 [M+H]+.

3.3.1.10 2-chloro-6,7-dimethoxy-N-[1-(propan-2-yl) piperidin-4-yl] quinazolin-4-amine (1j)

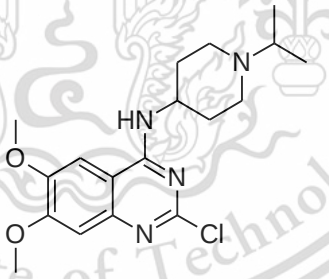

2,4-dichloro-6,7-dimethoxyquinazoline (1.0 eq, 1.93 mmol) and 1-(propan-2-yl) piperidin-4-amine (1.2 eq, 2.32 mmol), following the general synthetic procedure A to give the desired compound 1j as a yellow solid with 63.3% yield. ^{1}H-NMR (500 MHz, DMSO-d^6) δ 8.01 (d, *J* = 7.7 Hz, 1H), 7.65 (s, 1H), 7.06 (s, 1H), 3.89 (d, *J* = 4.0 Hz, 6H), 3.17 (s, 1H), 2.85 (d, *J* = 11.6 Hz, 2H), 2.73 (dt, *J* = 13.1, 6.6 Hz, 1H), 2.23 (t, *J* = 10.9 Hz, 2H), 1.93 (d, *J* = 9.2 Hz, 2H), 1.61 (q, *J* = 12.0 Hz, 2H), 1.00 (s, 3H), 0.98 (s, 3H). MS-ESI: m/z 365.1 [M+H]+.

3.3.1.11 2-chloro-6,7-dimethoxy-N-[1-benzylpiperidin-4-yl] quinazolin-4-amine (1k)

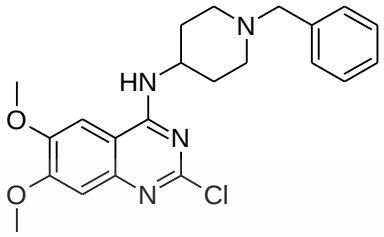

2,4-dichloro-6,7-dimethoxyquinazoline (1.0 eq, 1.93 mmol) and 1-benzylpiperidin-4-amine (1.2 eq, 2.32 mmol), following the general synthetic procedure A to give the desired compound 1k as a yellow solid with 99.1% yield. ^{1}H-NMR (500 MHz, DMSO-d^6) δ 8.00 (d, *J* = 7.7 Hz, 1H), 7.64 (s, 1H), 7.37 – 7.29 (m, 4H), 7.26 (td, *J* = 6.0, 2.5 Hz, 1H), 7.06 (s, 1H), 4.17 – 4.07 (m, 1H), 3.89 (d, *J* = 5.1 Hz, 6H), 3.51 (s, 2H), 2.88 (d, *J* = 11.7 Hz, 2H), 2.08 (t, *J* = 11.0 Hz, 2H), 1.91 (dd, *J* = 11.6, 2.3 Hz, 2H), 1.67 (qd, *J* = 12.1, 3.7 Hz, 2H) MS-ESI: m/z 413.1 [M+H]+.

3.3.1.12 1-methyl-4-(3-nitrobenzene-1-sulfonyl) piperazine (2a)

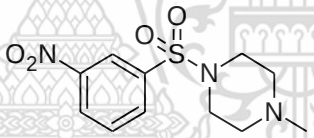

A mixture of 3-nitrobenzene-1-sulfonyl chloride (1.0 eq, 4.51 mmol) and 1-methylpiperazine (1.2 eq, 5.41 mmol) was stirred in DCM (20 ml.) at 0°C-room temperature, keep stirred the reaction for 4 h until its completion. The resulting mixture was evaporated, washed with 40 ml. saturated NaCl in water and extracted with ethyl acetate (3 x 20 ml). the organic layers were combined, dried over anhydrous Na_2SO_4, and concentrated in vacuum to give the compound **2a** as a yellow solid with 82.57%yield. ^{1}H-NMR (500 MHz, DMSO-d^6) δ 8.52 (dd, *J* = 6.7, 1.4 Hz, 1H), 8.33 (t, *J* = 1.6 Hz, 1H), 8.14 (d, *J* = 6.3 Hz, 1H), 7.92 (t, *J* = 6.4 Hz, 1H), 2.94 (s, 4H), 2.32 (t, *J* = 3.8 Hz, 4H), 2.10 (s, 3H). MS-ESI: m/z 286.1 [M+H]+.

3.3.1.13 1-methyl-4-(4-nitrobenzene-1-sulfonyl) piperazine (2b)

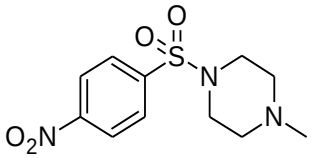

4-nitrobenzene-1-sulfonyl chloride (1.0 eq, 4.51 mmol) and 1-methylpiperazine (1.2 eq, 5.41 mmol), following the reaction procedure of compound **2a** to give the desired compound **2b** as a yellow solid with 91.76%yield. ^{1}H-NMR (500 MHz, DMSO-d^6) δ 8.42 (d, *J* = 1.5 Hz, 1H), 8.40 (d, *J* = 1.5 Hz, 1H), 7.97 (d, *J* = 1.6 Hz, 1H), 7.96 (d, *J* = 1.5 Hz, 1H), 2.93 (s, 4H), 2.33 (s, 4H), 2.11 (s, 3H) MS-ESI: m/z 286.2 [M+H]+.

3.3.1.14 3-(4-methylpiperazine-1-sulfonyl) aniline (3a)

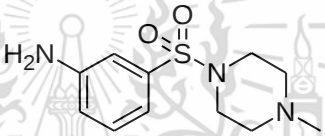

3.92 mmol of 1-methyl-4-(3-nitrobenzene-1-sulfonyl) piperazine **(2a)** was stirred in 20 ml of methanol, 100 mg of 10% of Pd/C was added, H_2 gas was flowed into the reaction mixture using small balloon, keep stirred for 2-4 h until its completion. The mixture was filtered using Celite545 and extracted with water/ethyl acetate (3 x 20 ml). the organic layers were combined, dried over anhydrous Na_2SO_4 and concentrated in vacuum to give the compound **3a** as a yellow solid with 95.53%yield. ^{1}H-NMR (500 MHz, DMSO-d^6) δ 7.20 (t, *J* = 6.3 Hz, 1H), 6.85 (s, 1H), 6.79 (d, *J* = 6.5 Hz, 1H), 6.74 (d, *J* = 6.6 Hz, 1H), 5.60 (s, 2H), 2.81 (s, 4H), 2.30 (s, 4H), 2.09 (s, 3H). MS-ESI: m/z 256.1 [M+H]+.

3.3.1.15 4-(4-methylpiperazine-1-sulfonyl) aniline (3b)

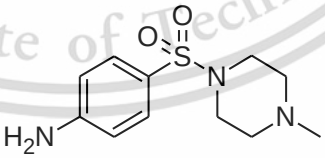

3.92 mmol of 1-methyl-4-(4-nitrobenzene-1-sulfonyl) piperazine **(2b),** following the reaction procedure of compound **3a** to give the desired compound **3b** as a yellow solid with 67.82%yield. ^{1}H-NMR (500 MHz, DMSO-d^6) δ 7.29 (d, *J* = 6.9 Hz, 2H), 6.60 (d, *J* = 7.0 Hz, 2H), 6.03 (s, 2H), 2.74 (s, 4H), 2.29 (s, 4H), 2.08 (s, 3H). MS-ESI: m/z 256.1 [M+H]+.

3.3.2 General synthesis procedure B

A mixture of 2,6-dichloro-9-methyl-9h-purine or 2,6-dichloropurine (1.0 eq) and amine (1.2 eq) was stirred for 10 min in n-butanol (10 ml), DIPEA (0.50 ml) was added in a solution, keep stirred the reaction at 90°C for 6 h until its completion. The product was precipitated, filtered, and concentrated under reduced pressure to afford the desired compound as a white solid.

3.3.2.1 N-benzyl-2-chloro-9-methyl-9H-purin-6-amine (22a)

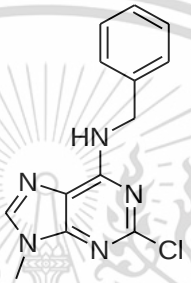

2,6-dichloro-9-methyl-9h-purine (1.0 eq) and benzyl amine (1.2 eq), following the general synthetic procedure B to give the desired compound 22a as a white solid with 92.68% yield. 1H-NMR (500 MHz, DMSO-d6) δ 8.73 (d, J = 4.1 Hz, 1H), 8.08 (s, 1H), 7.29 (dd, J = 6.7, 1.4 Hz, 3H), 7.26 (d, J = 6.2 Hz, 1H), 7.19 (t, J = 5.3 Hz, 1H), 4.60 (d, J = 4.8 Hz, 1H), 3.65 (s, 3H). MS-ESI: m/z 274.0 [M+H]+.

3.3.2.2 2-chloro-9-methyl-N-propyl-9H-purin-6-amine (22b)

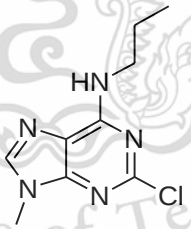

2,6-dichloro-9-methyl-9h-purine (1.0 eq) and propyl amine (1.2 eq), following the general synthetic procedure B to give the desired compound 22b as a white solid with 27.16% yield. 1H-NMR (500 MHz, DMSO-d6) δ 8.18 (s, 1H), 8.04 (s, 1H), 3.64 (s, 3H), 3.36 – 3.30 (m, 2H), 1.55 (dd, J = 11.6, 5.9 Hz, 2H), 0.85 (t, J = 5.9 Hz, 3H). MS-ESI: m/z 226.1 [M+H]+.

3.3.2.3 2-chloro-9-methyl-N-(2-methylpropyl)-9H-purin-6-amine (22c)

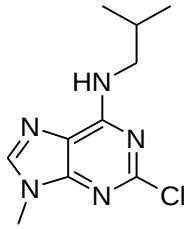

2,6-dichloro-9-methyl-9h-purine (1.0 eq) and isobutyl amine (1.2 eq), following the general synthetic procedure B to give the desired compound 22c as a white solid with 41.27% yield. 1H-NMR (500 MHz, DMSO-d6) δ 8.20 (s, 1H), 8.04 (s, 1H), 3.64 (s, 2H), 2.04 (s, 3H), 0.85 (s, 3H), 0.84 (s, 3H). MS-ESI: m/z 240.1 [M+H]+.

3.3.2.4 N-benzyl-2-chloro-9-(oxan-2-yl)-9H-purin-6-amine (32a)

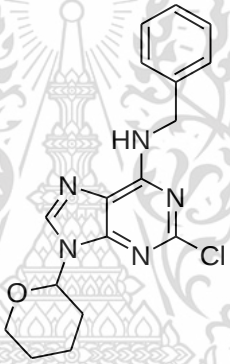

Compound 31a (1.0 eq) and benzyl amine (1.2 eq), following the general synthetic procedure B to give the desired compound 32a as a white solid with 85.44% yield. 1H-NMR (500 MHz, DMSO-d6) δ 9.63 – 9.59 (m), 8.84 (t, J = 4.7 Hz, 1H), 8.35 (s, 1H), 7.31 – 7.29 (m, 1H), 7.29 (s, 1H), 7.28 (s, 1H), 7.27 (s, 1H), 7.19 (t, J = 5.3 Hz, 1H), 5.52 (dd, J = 8.8, 1.7 Hz, 1H), 4.64 – 4.57 (m, 2H), 3.95 (d, J = 9.0 Hz, 1H), 1.89 (d, J = 8.3 Hz, 2H), 1.75 – 1.59 (m, 2H), 1.52 (t, J = 4.8 Hz, 2H), 1.47 – 1.34 (m, 2H). MS-ESI: m/z 344.2 [M+H]+.

3.3.2.5 N-[1-(propan-2-yl)piperidin-4-yl]-2-chloro-9-(oxan-2-yl)-9H-purin-6-amine (32b)

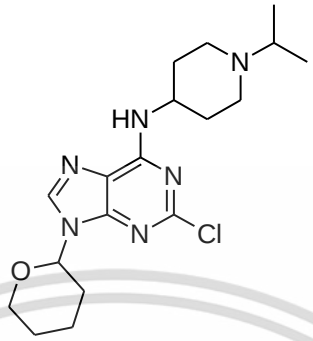

Compound 31a (1.0 eq) and 1-Isopropylpiperidin-4-amine (1.2 eq), following the general synthetic procedure B to give the desired compound 32b as a white solid with 84.88% yield. 1H-NMR (500 MHz, DMSO-d6) δ 8.36 (s, 1H), 5.52 (d, J = 8.9 Hz, 1H), 3.95 (d, J = 9.3 Hz, 1H), 3.68 – 3.61 (m, 1H), 3.04 (s, 4H), 2.83 (s, 1H), 2.17 (d, J = 10.9 Hz, 2H), 1.89 (t, J = 10.7 Hz, 4H), 1.78 (s, 1H), 1.69 (s, 2H), 1.52 (s, 3H), 1.07 (s, 3H), 0.95 (d, J = 5.0 Hz, 2H). MS-ESI: m/z 379.3 [M+H]+.

3.3.2.6 2-chloro-N-(1-benzylpiperidin-4-yl)-9-(oxan-2-yl)-9H-purin-6-amine (32c)

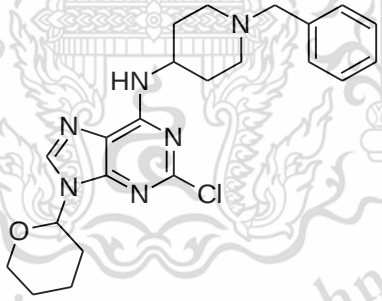

Compound 31a (1.0 eq) and 4-Amino-1-benzylpiperidine (1.2 eq), following the general synthetic procedure B to give the desired compound 32c as a white solid with 72.33% yield. 1H-NMR (500 MHz, DMSO-d6) δ 8.37 (s, 1H), 8.24 (s, 1H), 7.32 (d, J = 5.9 Hz, 4H), 7.29 (s, 1H), 3.99 (d, J = 9.1 Hz, 2H), 3.70 (dd, J = 9.5, 5.1 Hz, 1H), 3.52 (s, 2H), 3.47 (s, 3H), 3.00 – 2.92 (m, 1H), 2.81 (d, J = 12.2 Hz, 2H), 1.99 – 1.93 (m, 3H), 1.86 (d, J = 9.8 Hz, 2H), 1.70 (s, 2H), 1.55 (d, J = 2.9 Hz, 2H). MS-ESI: m/z 427.3 [M+H]+.

3.3.3 General synthesis procedure C

A solution of product in general synthetic procedure A (1.0 eq) and amine (1.2 eq) was stirred in isopropanol (10 ml), 1M HCl (1.50 ml) was slowly added, the resulting mixture was stirred at 90°C for 8 h until its completion. The reaction mixture was filtered and concentrated under reduced pressure. The residue was extracted with water/EtOAc 3 times, the organic layers were combined, dried over anhydrous Na_2SO_4 and evaporated. Finally, column chromatography was used to purify with DCM/EtOAc = 3/1 to afford the desired compound as the white or/and yellow solid.

3.3.3.1 2-(3-(1-methylpiperazinesulfonylamino))-4-(benzylamino) quinazoline (4)

N-benzyl-2-chloroquinazolin-4-amine 1b (1.0 eq) with 3-[4-methylpiperazin-1-yl)-sulfonyl] aniline 3a (1.2 eq) following the general synthetic procedure C to give a desired compound 4 in 168 mg, 92.49% yield as a white solid. 1H-NMR NMR (500 MHz, DMSO-d6) δ 8.41 (d, 1H, J = 6.5 Hz), 8.23 (s, 1H), 7.84 (t, 1H, J = 6.1 Hz), 7.77 (d, 1H, J = 6.2 Hz), 7.60 (t, 3H, J = 6.4 Hz), 7.48 (dd, 2H, J = 12.2, 6.1 Hz), 7.32 (s, 1H), 7.31 (d, 2H, J = 2.6 Hz), 7.28 (d, 2H, J = 6.2 Hz), 7.23 (t, 1H, J = 5.5 Hz), 4.83 (d, 2H, J = 4.6 Hz), 3.59 (d, 2H, J = 9.4 Hz), 3.06 (s, 2H), 2.68 (s, 3H), 2.64 (s, 2H). ^{13}C-NMR (101 MHz, DMSO-d6) δ 163.54, 160.82, 138.81, 138.13, 137.70, 136.09, 135.20, 130.89, 128.95, 127.90, 127.79, 125.78, 124.20, 120.78, 118.79, 110.72, 52.26, 49.07, 43.45, 42.72. HRMS (ESI) calculated for C26H29N6O2S 489.2067, found 489.2084 [M+H]+

3.3.3.2 2-(3-(1-methylpiperazinesulfonylamino))-4-(2-thiophenemethylamino) quinazoline (5)

2-chloro-N-[(thiophen-2-yl)methyl] quinazolin-4-amine 1a (1.0 eq) with 3-[4-methylpiperazin-1-yl)-sulfonyl] aniline 3a (1.2 eq) following the general synthetic procedure C to give a desired compound 5 in 54 mg, 80.26% yield as a white solid. 1H-NMR (500 MHz, DMSO-d6) δ 8.31 (d, 1H, J = 6.0 Hz), 7.88 (d, 1H, J = 6.4 Hz), 7.66 (t, 1H, J = 6.4 Hz), 7.60 (d, 1H, J = 6.6 Hz), 7.50 (s, 1H), 7.45 (s, 1H), 7.36 (dd, 1H, J = 4.1, 0.9 Hz), 7.03 (d, 1H, J = 2.4 Hz), 6.92 (dd, 1H, J = 4.0, 2.8 Hz), 4.97 (d, 2H, J = 4.6 Hz), 3.65 (d, 2H, J = 9.8 Hz), 3.08 (s, 2H), 2.70 (s, 3H), 2.65 (t, 2H, J = 10.0 Hz), 2.62 – 2.56 (m, 1H), 1.01 (t, 3H,

J = 5.6 Hz). ^{13}C-NMR (101 MHz, DMSO-d6) δ HRMS (ESI) calculated for $C_{24}H_{26}N_6O_2S_2$ 495.1631, found 495.1634 [M+H]+

3.3.3.3 2-(4-(1-methylpiperazinesulfonylamino))-4-(benzylamino) quinazoline (6)

N-benzyl-2-chloroquinazolin-4-amine 1b (1.0 eq) and 4-[4-methylpiperazin-1-yl)-sulfonyl] aniline 3b (1.2 eq), following the general synthetic procedure C, to give a desired compound 6 with 81.15% yield as a white solid. 1H-NMR (500 MHz, DMSO-d6) δ 10.87 (s, 1H), 8.47 (d, 1H, J = 6.5 Hz), 7.85 (t, 1H, J = 6.2 Hz), 7.72 (d, 2H, J = 6.7 Hz), 7.63 (s, 1H), 7.61 (s, 1H), 7.58 (d, 1H, J = 6.7 Hz), 7.50 (t, 1H, J = 6.1 Hz,), 7.37 (d, 2H, J = 5.8 Hz), 7.33 (t, 2H, J = 6.1 Hz), 7.25 (t, 1H, J = 5.8 Hz), 4.81 (d, 2H, J = 4.6 Hz), 3.73 (d, 2H, J = 9.5 Hz), 3.42 (d, 2H, J = 9.5 Hz), 3.11 (s, 2H), 2.70 (s, 3H), 2.60 (m, 2H). ^{13}C-NMR (101 MHz, DMSO-d6) δ 161.02, 151.87, 142.68, 138.04, 136.16, 129.23, 129.01, 127.75, 127.59, 125.79, 125.03, 121.55, 118.57, 111.10, 52.02, 45.48, 43.58, 42.39. HRMS (ESI) calculated for $C_{26}H_{29}N_6O_2S$ 489.2067, found 489.2068 [M+H]+

3.3.3.4 2-(3-(1-methylpiperazinesulfonylamino))-4-(propylamino) quinazoline (7)

2-chloro-N-propylquinazolin-4-amine 1c (1.0 eq.) and 3-[4-methylpiperazin-1-yl)-sulfonyl] aniline 3a (1.2 eq.), following the general synthetic procedure C, to give a desired compound 7 with 66.85% yield as a white solid. 1H-NMR (500 MHz, DMSO-d6) δ 9.42 (s, 1H), 8.62 (s, 1H), 8.10 (dd, 2H, J = 12.0, 5.2 Hz), 7.99 (d, 1H, J = 5.7 Hz), 7.57 (t, 1H, J = 6.1 Hz), 7.46 (t, 1H, J = 6.4 Hz), 7.34 (d, 1H, J = 6.5 Hz), 7.17 (t, 2H, J = 5.6 Hz), 3.51 (dd, 2H, J = 10.8, 5.0 Hz), 2.91 (s, 4H), 2.34 (s, 4H), 2.09 (s, 3H), 1.66 (dd, 2H, J = 11.6, 5.8 Hz), 0.93 (t, 3H, J = 5.9 Hz). ^{13}C-NMR (101 MHz, DMSO-d6) δ 163.75, 160.76, 155.65, 141.56, 134.88, 134.16, 130.34, 124.46, 123.67, 123.19, 120.79, 118.01, 111.66, 52.78, 49.07, 46.45, 44.33, 43.56, 43.14, 22.02, 11.67. HRMS (ESI) calculated for $C_{22}H_{29}N_6O_2S$ 441.2067, found 441.2093 [M+H]+

3.3.3.5 2-(4-(1-methylpiperazinesulfonylamino))-4-(propylamino) quinazoline (8)

2-chloro-N-propylquinazolin-4-amine 1c (1.0 eq.) and 4-[4-methylpiperazin-1-yl)-sulfonyl] aniline 3b (1.2 eq.), following the general synthetic procedure C, to give a desired compound 8 with 8.05% yield as a yellow solid. 1H-NMR (500 MHz, DMSO-d6) δ 9.57 (s, 1H), 8.18 (t, 1H, J = 5.0 Hz), 8.16 (d, 2H, J = 7.1 Hz), 8.09 (d, 1H, J = 6.2 Hz), 7.58 (t, 1H, J = 5.8 Hz), 7.55 (d, 2H, J = 7.1 Hz), 7.43 (d, 1H, J = 6.5 Hz), 7.19 (t, 1H, J = 5.7 Hz), 3.50 (dd, 2H, J = 11.0, 4.9 Hz), 2.81 (s, 4H), 2.30 (s, 4H), 2.08 (s, 3H), 1.67 (dd, 2H, J = 11.7, 5.9 Hz), 0.93 (t, 3H, J = 5.9 Hz). ^{13}C-NMR (101 MHz, DMSO-d6) δ HRMS (ESI) calculated for $C_{22}H_{29}N_6O_2S$ 441.2067, found 441.2050 [M+H]+

3.3.3.6 2-(3-(1-methylpiperazinesulfonylamino))-4-(isopropylamino) quinazoline (9)

2-chloro-N-(2-methylpropyl) quinazolin-4-amine 1d (1.0 eq.) with 3-[4-methylpiperazin-1-yl)-sulfonyl] aniline 3a (1.2 eq.), following the general synthetic procedure C, given the desired product 9 with 25.92% yield as a white solid. 1H-NMR (500 MHz, DMSO-d6) δ 9.38 (s,1H), 8.55 (s, 1H), 8.15 – 8.00 (m, 3H), 7.57 (t, 1H, J = 6.0 Hz), 7.46 (t, 1H, J = 6.3 Hz), 7.34 (d, 1H, J = 6.6 Hz), 7.16 (d, 2H, J = 5.9 Hz), 3.39 – 3.35 (m, 2H), 2.90 (s, 4H), 2.81 (s, 1H), 2.34 (s, 4H), 2.09 (s, 3H), 0.93 (s, 3H), 0.92 (s, 3H). ^{13}C-NMR (101 MHz, DMSO-d6) δ 163.69, 160.95, 157.00, 150.78, 149.44, 135.66, 135.46, 133.56, 130.41, 125.41, 123.36, 122.89, 119.04, 112.25, 53.58, 49.07, 45.79, 45.22, 27.94, 20.47. HRMS (ESI) calculated for $C_{23}H_{31}N_6O_2S$ 455.2224, found 455.2214 [M+H]+

3.3.3.7 2-(4-(1-methylpiperazinesulfonylamino))-4-(isopropylamino) quinazoline (10)

2-chloro-N-(2-methylpropyl) quinazolin-4-amine 1d (1.0 eq.) and 4-[4-methylpiperazin-1-yl)-sulfonyl] aniline 3b (1.2 eq.), following the general synthetic procedure C, given the desired product 10 with 21.78% yield as a white solid. 1H-NMR (500 MHz, DMSO-d6) NMR δ 9.57 (s, 1H), 8.22 (t, 1H, J = 4.4 Hz), 8.13 (t, 3H, J = 6.2 Hz), 7.61 – 7.56 (m, 1H), 7.55 (d, 2H, J = 7.1 Hz), 7.42 (dd, 1H, J = 6.5, 3.2 Hz), 7.21 – 7.18 (m, 1H), 2.82 (s, 4H), 2.61 – 2.57 (m, 2H), 2.32 (dd, 4H, J = 2.8, 1.3 Hz), 2.09 (s, 3H), 0.94 (s, 3H),

0.92 (s, 3H). ^{13}C-NMR (101 MHz, DMSO-d6) δ 163.65, 160.85, 156.77, 150.77, 146.15, 133.55, 128.87, 125.72, 123.16, 122.91, 118.45, 112.14, 53.57, 49.07, 48.69, 45.79, 45.23, 27.75, 20.53. HRMS (ESI) calculated for $C_{23}H_{31}N_6O_2S$ 455.2224, found 455.2242 [M+H]+

3.3.3.8 2-(3-sulfonylamino)-4-(propylamino)-6,7-dimethoxyquinazoline (11)

2-chloro-6,7-dimethoxy-N-propylquinazolin-4-amine 1h (1.0 eq) and 3-aminobenzene sulfonamide (1.2 eq), following the general synthetic procedure C to give a desired compound 11 with 85.03% yield as a white solid. 1H-NMR (500 MHz, DMSO-d6) δ 10.40 (s, 1H), 8.18 (s, 1H), 7.77 (s, 1H), 7.74 (d, 1H, J = 5.8 Hz), 7.57 (s, 1H), 7.57 – 7.54 (m, 1H), 7.37 (s, 2H), 7.05 (s, 1H), 3.88 (s, 3H), 3.84 (s, 3H), 1.63 (dd, 2H, J = 11.6, 5.9 Hz), 0.99 (s, 2H), 0.89 (t, 3H, J = 5.9 Hz). ^{13}C-NMR (101 MHz, DMSO-d6) δ 159.70, 155.92, 150.87, 147.74, 145.32, 138.41, 135.23, 130.05, 124.56, 121.64, 118.57, 105.13, 103.32, 99.27, 56.99, 56.71, 43.97, 26.00, 22.21. HRMS (ESI) calculated for $C_{19}H_{24}N_5O_4S$ 418.1544, found 418.1545 [M+H]+

3.3.3.9 2-(3-sulfonylamino)-4-(isopropylamino)-6,7-dimethoxyquinazoline (12)

2-chloro-6,7-dimethoxy-N-isopropylquinazolin-4-amine 1i (1.0 eq) and 3-aminobenzene sulfonamide (1.2 eq), following the general synthetic procedure C to give a desired compound 12 with 71.26% yield as a white solid. 1H-NMR (500 MHz, DMSP-d6) δ 12.45 (d, 1H, J = 28.8 Hz), 10.45 (s, 1H), 9.43 (d, 1H, J = 32.7 Hz), 8.08 (s, 1H), 7.82 (s, 1H), 7.79 (d, 1H, J = 6.0 Hz), 7.59 (d, 1H, J = 6.2 Hz), 7.58 – 7.55 (m, 1H), 7.38 (s, 2H), 7.04 (s, 1H), 3.89 (s, 3H), 3.85 (s, 3H), 3.39 – 3.36 (m, 2H), 1.97 (dt, 1H, J = 10.9, 5.4 Hz), 0.89 (s, 3H), 0.88 (s, 3H). ^{13}C-NMR (101 MHz, DMSO-d6) δ 163.70, 159.83, 155.78, 150.77, 147.64, 144.44, 138.18, 135.82, 130.18, 125.48, 123.28, 121.80, 119.11, 103.23, 56.61, 56.56, 49.07, 28.08, 20.33. HRMS (ESI) calculated for $C_{20}H_{26}N_5O_4S$ 432.1700, found 432.1700 [M+H]+

3.3.3.10 2-(4-sulfonylamino)-4-(isopropylamino)-6,7-dimethoxyquinazoline (13)

2-chloro-6,7-dimethoxy-N-isopropylquinazolin-4-amine 1i (1.0 eq) and 4-aminobenzene sulfonamide (1.2 eq), following the general synthetic procedure C to give

a desired compound 13 with 54.85% yield as a white solid. 1H-NMR (500 MHz, DMSO-d6) δ 12.25 (s, 1H), 10.26 (s, 1H), 9.35 (s, 1H), 7.78 (s, 4H), 7.31 (s, 1H), 7.05 (s, 1H), 3.88 (s, 3H), 3.85 (s, 3H), 3.46 (s, 1H), 2.02 (dd, 1H, J = 10.8, 5.4 Hz), 0.94 (s, 3H), 0.92 (s, 3H). ^{13}C-NMR (101 MHz, DMSO-d6) δ 163.81, 159.70, 155.78, 150.35, 147.72, 141.08, 138.79, 135.57, 126.91, 121.55, 103.86, 103.24, 99.41, 56.59, 56.50, 49.54, 49.07, 27.95, 20.41. HRMS (ESI) calculated for $C_{20}H_{26}N_5O_4S$ 432.1700, found 432.1718 [M+H]+

3.3.3.11 2-(3-sulfonylamino)-4-(isopropylpiperidin-4-amino) quinazoline (24)

2-chloro-N-[1-(propan-2-yl) piperidin-4-yl] quinazolin-4-amine 1e (1.0 eq) and 3-aminobenzene sulfonamide (1.2 eq), following the general synthetic procedure C to give a desired compound 24 with 83.72% yield as a white solid. 1H-NMR (500 MHz, DMSO-d6) δ 10.99 (s, 1H), 10.55 (s, 1H), 9.86 (d, J = 6.9 Hz, 1H), 8.66 – 8.59 (m, 2H), 7.89 (t, J = 7.7 Hz, 1H), 7.66 (t, J = 7.6 Hz, 2H), 7.60 – 7.55 (m, 2H), 7.54 (s, 2H), 7.53 – 7.48 (m, 1H), 4.53 (s, 1H), 3.13 (dd, J = 22.8, 10.6 Hz, 3H), 2.30 (dd, J = 24.7, 11.5 Hz, 3H), 2.14 (d, J = 12.8 Hz, 2H), 1.33 (s, 3H), 1.31 (s, 3H). ^{13}C-NMR (101 MHz, DMSO-d6) δ 160.54, 151.70, 145.03, 138.14, 136.21, 130.41, 125.44, 125.31, 124.21, 121.81, 118.17, 117.90, 110.73, 57.52, 48.18, 46.85, 28.13, 16.82. HRMS (ESI) calculated for $C_{22}H_{29}N_6O_2S$ 441.2067, found 441.2056 [M+H]+

3.3.3.12 2-(3-(1-methylpiperazinesulfonylamino))-4-(isopropylpiperidin-4-amino) quinazoline (25)

2-chloro-N-[1-(propan-2-yl) piperidin-4-yl] quinazolin-4-amine 1e (1.0 eq) and 3-[4-methylpiperazin-1-yl)-sulfonyl] aniline 3a (1.2 eq.), following the general synthetic procedure C to give a desired compound 25 with 84.66% yield as a white solid. 1H-NMR (500 MHz, DMSO-d6) δ 10.49 (s, 1H), 9.59 (s, 1H), 8.52 (d, 1H, J = 6.5 Hz), 8.38 (s, 1H), 7.83 (t, 1H, J = 6.1 Hz), 7.77 (d, 1H, J = 6.5 Hz), 7.71 (t, 1H, J = 6.3 Hz), 7.52 (d, 2H, J = 6.5 Hz), 7.44 (t, 1H, J = 6.1 Hz), 3.44 (dd, 12H, J = 16.7, 7.6 Hz), 2.98 (dd, 2H, J = 18.4, 8.5 Hz), 2.70 (s, 3H), 2.18 (dd, 4H, J = 19.3, 9.6 Hz), 1.26 (s, 3H), 1.25 (s, 3H). ^{13}C-NMR (101 MHz, DMSO-d6) δ 160.62, 159.66, 159.40, 135.07, 130.94, 130.64, 126.53, 124.34, 124.08, 121.54, 120.89, 118.53, 116.16, 57.51, 52.16, 47.09, 43.74, 28.24, 16.82. HRMS (ESI) calculated for $C_{27}H_{38}N_7O_2S$ 524.2802, found 524.2819 [M+H]+

3.3.3.13 2-(3-sulfonylamino)-4-(N, N-dimethylethylenediamino) quinazoline (26)

N2-(2-chloroquinazolin-4-yl)-N1, N1-dimethylethane-1,2-diamine 1f (1.0 eq.) and 3-aminobenzene sulfonamide (1.2 eq.), following the general synthetic procedure C to give a desired compound 26 with 78.03% yield as a white solid. 1H-NMR (500 MHz, DMSO-d6) δ 11.10 (s, 1H), 10.15 (s, 1H), 10.04 (s, 1H), 8.46 (d, J = 8.2 Hz, 1H), 8.38 (s, 1H), 7.88 (t, J = 7.4 Hz, 1H), 7.72 – 7.67 (m, 1H), 7.65 (s, 2H), 7.59 (d, J = 8.1 Hz, 1H), 7.51 (d, J = 7.9 Hz, 1H), 7.49 (s, 2H), 3.97 (d, J = 5.5 Hz, 2H), 2.81 (s, 6H). ^{13}C-NMR (101 MHz, DMSO-d6) δ 161.41, 160.06, 159.73, 145.17, 138.37, 136.01, 135.44, 130.27, 127.41, 125.20, 122.81, 119.11, 115.79, 111.14, 55.38, 42.85, 37.21. HRMS (ESI) calculated for $C_{18}H_{23}N_6O_2S$ 387.1598, found 387.1613 [M+H]+

3.3.3.14 2-(3-(1-methylpiperazinesulfonylamino))-4-(N, N-dimethylethylenediamino) quinazoline (27)

N2-(2-chloroquinazolin-4-yl)-N1, N1-dimethylethane-1,2-diamine 1f (1.0 eq.) and 3-[4-methylpiperazin-1-yl)-sulfonyl] aniline 3a (1.2 eq.), following the general synthetic procedure C to give a desired compound 27 with 36.67% yield as a white solid. 1H-NMR (500 MHz, DMSO-d6) δ 11.07 (s, 1H), 10.32 (s, 1H), 8.56 – 8.47 (m, 1H), 8.22 (s, 1H), 7.85 (dt, 1H, J = 11.6, 6.5 Hz), 7.71 (t, , 1HJ = 6.4 Hz), 7.60 (t, 1H, J = 6.3 Hz), 7.53 (d, 1H, J = 5.8 Hz), 7.46 (t, 1H, J = 6.1 Hz), 3.92 (dd, 2H, J = 8.8, 4.3 Hz), 3.76 (d, 2H, J = 8.7 Hz), 3.39 (s, 4H), 3.12 (s, 2H), 2.77 (s, 6H), 2.75 (s, 1H), 2.71 (s, 1H), 2.70 (d, 3H, J = 5.2 Hz). ^{13}C-NMR (101 MHz, DMSO-d6) δ HRMS (ESI) calculated for $C_{23}H_{32}N_7O_2S$ 470.2333, found 470.2353 [M+H]+

3.3.3.15 2-(3-sulfonylamino)-4-(benzylpiperidin-4-amino) quinazoline (28)

N-(1-benzylpiperidin-4-yl)-2-chloroquinazolin-4-amine 1g (1.0 eq.) and 3-aminobenzene sulfonamide (1.2 eq), following the general synthetic procedure C to give a desired compound 28 with 30.12% yield as a white solid. 1H-NMR (500 MHz, DMSO-d6) δ 11.12 (s, 1H), 10.85 (s, 1H), 8.54 (d, 1H, J = 6.6 Hz), 8.35 (s, 1H), 7.83 (t, 1H, J = 6.2 Hz), 7.68 – 7.65 (m, 1H), 7.61 (s, 1H), 7.60 (s, 1H), 7.60 (s, 1H), 7.57 (s, 2H), 7.54 (d, 1H, J = 6.6 Hz), 7.44 – 7.43 (m, 3H), 4.44 – 4.35 (m, 1H), 4.21 (d, 2H, J = 4.0 Hz), 3.73 (t, 1H), 3.04 (dd,

2H,J = 18.1, 8.1 Hz), 2.22 – 2.12 (m, 2H), 2.06 (d, 2H, J = 10.7 Hz). ^{13}C-NMR (101 MHz, DMSO-d6) δ 160.54, 145.16, 136.20, 132.02, 130.40, 130.24, 130.04, 129.50, 129.32, 125.36, 124.83, 122.03, 118.70, 110.86, 59.79, 50.88, 48.28, 28.09. HRMS (ESI) calculated for $C_{26}H_{29}N_6O_2S$ 489.2067, found 489.2073 [M+H]+

3.3.3.16 2-(3-sulfonylamino)-4-(isopropylpiperidin-4-amino)-6,7-dimethoxyquinazoline (29)

2-chloro-6,7-dimethoxy-N-[1-(propan-2-yl) piperidin-4-yl] quinazolin-4-amine 1j (1.0 eq.) and 3-aminobenzene sulfonamide (1.2 eq), following the general synthetic procedure C to give a desired compound 29 with 88.54% yield as a white solid. 1H-NMR (500 MHz, DMSO-d6) δ 10.87 (s, 1H), 10.51 (s, 1H), 10.50 (s, 1H), 9.65 (s, 1H), 8.57 (s, 1H), 8.13 (s, 1H), 7.64 (s, 2H), 7.53 (s, 2H), 7.04 (s, 1H), 3.95 (s, 3H), 3.93 (s, 3H), 3.13 (dd, J = 21.0, 10.2 Hz, 4H), 2.32 (dd, J = 22.1, 10.7 Hz, 4H), 2.15 (d, J = 12.5 Hz, 2H), 1.33 (s, 3H), 1.32 (s, 3H). ^{13}C-NMR (101 MHz, DMSO-d6) δ 159.51, 156.25, 150.67, 147.80, 145.00, 130.33, 124.04, 117.87, 111.36, 105.70, 103.27, 99.09, 57.54, 57.25, 56.76, 46.94, 28.38, 16.87. HRMS (ESI) calculated for $C_{24}H_{33}N_6O_4S$ 501.2279, found 501.2315 [M+H]+

3.3.3.17 2-(3-(1-methylpiperazinesulfonylamino))-4-(isopropylpiperidin-4-amino)-6,7-dimethoxyquinazoline (30)

2-chloro-6,7-dimethoxy-N-[1-(propan-2-yl) piperidin-4-yl] quinazolin-4-amine 1j (1.0 eq.) and 3-[4-methylpiperazin-1-yl)-sulfonyl] aniline 3a (1.2 eq), following the general synthetic procedure C to give a desired compound 20 with 30.29% yield as a white solid. 1H-NMR (500 MHz, DMSO-d6) δ 9.20 (s, 1H), 8.35 (s, 1H), 8.15 (s, 1H), 7.53 (s, 1H), 7.50 (s, 1H), 7.45 (t, 1H, J = 6.4 Hz), 7.14 (d, 1H, J = 6.6 Hz), 6.76 (s, 1H), 4.20 (s, 1H), 3.83 (s, 3H), 3.81 (s, 3H), 2.91 (s, 4H), 2.85 (s, 2H), 2.69 (s, 2H), 2.33 (s, 4H), 2.09 (s, 3H), 1.97 (s, 2H), 1.62 (s, 2H), 1.01 (s, 6H). ^{13}C-NMR (101 MHz, DMSO-d6) δ 163.68, 159.08, 156.20, 154.50, 147.72, 146.30, 142.50, 135.52, 129.94, 123.14, 119.44, 118.82, 117.06, 105.45, 104.86, 102.95, 56.35, 55.91, 54.89, 53.64, 49.07, 47.40, 45.93, 45.28, 31.45, 17.83. HRMS (ESI) calculated for $C_{29}H_{42}N_7O_4S$ 584.3014, found 584.3032 [M+H]+

3.3.3.18 2-(3-sulfonylamino)-4-(benzylpiperidin-4-amino)-6,7-dimethoxyquinazoline (34)

2-chloro-6,7-dimethoxy-N-[1-benzylpiperidin-4-yl] quinazolin-4-amine 1k (1.0 eq.) and 3-aminobenzene sulfonamide (1.2 eq), following the general synthetic procedure C to give a desired compound 21 with 79.41% yield as a white solid. 1H-NMR (500 MHz, DMSO-d6) δ 10.77 (s, 2H), 9.41 (s, 1H), 8.40 (s, 1H), 7.97 (s, 1H), 7.65 (dd, J = 14.5, 5.4 Hz, 3H), 7.62 – 7.58 (m, 4H), 7.51 – 7.47 (m, 3H), 7.03 (s, 1H), 4.42 (dd, J = 13.4, 7.2 Hz, 1H), 4.27 (s, 2H), 3.93 (s, 3H), 3.91 (s, 3H), 3.10 (s, 2H), 2.14 (s, 4H). ^{13}C-NMR (101 MHz, DMSO-d6) δ HRMS (ESI) calculated for $C_{28}H_{33}N_6O_4S$ 549.2279, found 549.2306 [M+H]+

3.3.4 General synthesis procedure D

A solution of 2,6-dichloropurine (1.0 eq) in ethyl acetate (5 ml), p-toluene sulfonic acid (0.1 eq, 0.04 mmol) in ethyl acetate was added, 3,4-dihydro-2H-pyran (2.0 eq, 0.78 mmol) was slowly dropped. The reaction mixture was stirred at 70℃ for 4 h until its completion. The resulting mixture was concentrated under reduced pressure and extracted with water/EtOAc (3 x 20 ml), the organic layers were combined and dried over anhydrous Na_2SO_4, purified by column chromatography with DCM/EtOAc = 3/1 to give the desired compound as a white solid.

3.3.4.1 2,6-dichloro-9-(oxan-2-yl)-9H-purine (31a)

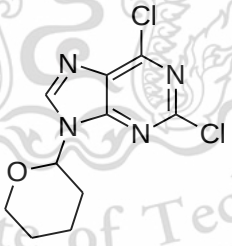

31a as the intermediate, following the general synthetic procedure D, given the desired product 31a as a white solid with 90.63% yield. 1H-NMR (500 MHz, DMSO-d6) δ 8.92 (s, 1H), 5.70 (dd, 1H, J = 8.7, 1.7 Hz), 3.98 (d, 1H, J = 8.9 Hz), 3.70 (dd, 1H, J = 11.7, 9.2 Hz), 2.22 (dt, 1H, J = 8.7, 6.9 Hz), 1.95 (t, 2H, J = 10.7 Hz), 1.78 – 1.63 (m, 2H), 1.55 (s, 1H). MS-ESI: m/z 274.1 [M+H]+.

3.3.5 General synthesis procedure E

The substitution reaction at 2 position of purine was performed via Buchwald–Hartwig reaction. A mixture of product in general synthetic procedure B or/and D (1.0 eq) and amine (1.2 eq) was suspended in anhydrous 1,4-dioxane (5 ml), $Pd_2(dba)_3$ (0.1 eq), Xphos (0.2 eq) were added in the solution under N2 atmosphere, the reaction was stirred for 10 min. K_2CO_3 (3.0 eq) was added, keep stirred the reaction at 110°C for overnight. Crude was filtered with Cerite545 and concentrated under reduced pressure, the residue was extracted with water/EtOAc 3 times, the organic layers were combined, dried over anhydrous Na_2SO_4 and evaporated. Finally, column chromatography was used to purify with DCM/EtOAc/TEA = 50/50/3 to afford the desired product as a yellow or/and dark brown solid.

3.3.5.1 2-(3-(1-methylpiperazinesulfonylamino))-6-(benzylamino)-9-methyl-9H-purine (14)

N-benzyl-2-chloro-9-methyl-9H-purin-6-amine 22a (1.0 eq.) and 3-[4-methylpiperazin-1-yl)-sulfonyl] aniline 3a (1.2 eq.), following the general synthetic procedure E, the desired product 14 was obtained with 56.68% yield as a yellow solid. 1H-NMR (500 MHz, DMSO-d6) δ 9.42 (s, 1H), 8.59 (s, 1H), 8.13 (s, 1H), 7.84 (s, 2H), 7.39 (t, 1H, J = 6.4 Hz), 7.32 (d, 2H, J = 5.8 Hz), 7.25 (t, 2H, J = 6.1 Hz), 7.16 (t, 1H, J = 5.8 Hz), 7.11 (d, 1H, J = 6.2 Hz), 4.72 (s, 2H), 3.63 (s, 3H), 2.78 (s, 4H), 2.25 (s, 4H), 2.06 (s, 3H). ^{13}C-NMR (101 MHz, DMSO-d6) δ 156.23, 143.01, 139.98, 135.28, 129.66, 128.70, 127.70, 127.13, 122.51, 119.18, 116.56, 53.97, 46.27, 45.79, 29.69. HRMS (ESI) calculated for $C_{24}H_{29}N_8O_2S$ 493.2129, found 493.2158 [M+H]+

3.3.5.2 2-(4-(1-methylpiperazinesulfonylamino))-6-(benzylamino)-9-methyl-9H-purine (15)

N-benzyl-2-chloro-9-methyl-9H-purin-6-amine 22a (1.0 eq.) and 4-[4-methylpiperazin-1-yl)-sulfonyl] aniline 3b (1.2 eq.), following the general synthetic procedure E, the desired product 15 was obtained with 30.69% yield as a yellow solid. 1H-NMR (500 MHz, DMSO-d6) δ 9.56 (s, 1H), 8.26 (s, 1H), 7.92 (d, 2H, J = 4.6 Hz), 7.87 (s, 1H), 7.44 (d, 2H, J = 6.6 Hz), 7.34 (d, 2H, J = 6.0 Hz), 7.26 (t, 2H, J = 6.1 Hz), 7.16 (t, 1H, J = 5.8 Hz), 4.69 (s, 2H), 3.65 (s, 3H), 2.79 (s, 4H), 2.31 (s, 4H), 2.09 (s, 3H). ^{13}C-NMR (101 MHz,

DMSO-d6) δ 155.86, 151.06, 146.60, 140.46, 128.97, 128.71, 127.42, 127.07, 124.89, 117.62, 54.06, 46.27, 45.83, 29.83. HRMS (ESI) calculated for $C_{24}H_{29}N_8O_2S$ 493.2129, found 493.2117 [M+H]+

3.3.5.3 2-(3-(1-methylpiperazinesulfonylamino))-6-(propylamino)-9-methyl-9H-purine (16)

2-chloro-9-methyl-N-propyl-9H-purin-6-amine 22b (1.0 eq.) and 3-[4-methylpiperazin-1-yl)-sulfonyl] aniline 3a (1.2 eq.), following the general synthetic procedure E, the desired product 16 was obtained with 55.04% yield as a dark brown solid. 1H-NMR (500 MHz, DMSO-d6) δ 9.38 (s, 1H), 8.65 (s, 1H), 7.89 (s, 1H), 7.81 (s, 1H), 7.56 (s, 1H), 7.43 (t, 1H, J = 6.4 Hz), 7.13 (d, 1H, J = 6.3 Hz), 3.62 (s, 3H), 2.87 (s, 4H), 2.32 (s, 4H), 2.08 (s, 3H), 1.59 (dd, 2H, J = 11.6, 5.8 Hz), 1.19 (t, 2H, J = 5.8 Hz), 0.88 (t, 3H, J = 5.9 Hz). ^{13}C-NMR (101 MHz, DMSO-d6) δ 163.50, 156.18, 154.96, 142.69, 139.79, 135.36, 129.84, 122.64, 119.37, 116.42, 114.33, 53.63, 49.06, 45.93, 45.32, 29.57, 22.76, 11.65. HRMS (ESI) calculated for $C_{20}H_{28}KN_8O_2S$ 483.1688, found 483.1703 [M+H]+

3.3.5.4 2-(4-(1-methylpiperazinesulfonylamino))-6-(propylamino)-9-methyl-9H-purine (17)

2-chloro-9-methyl-N-propyl-9H-purin-6-amine 22b (1.0 eq.) and 4-[4-methylpiperazin-1-yl)-sulfonyl] aniline 3b (1.2 eq.), following the general synthetic procedure E, the desired product 17 was obtained with 68.03% yield as a dark brown solid. 1H-NMR (500 MHz, DMSO-d6) δ 9.56 (s, 1H), 8.08 (d, 2H, J = 7.1 Hz), 7.83 (s, 1H), 7.67 (s, 1H), 7.52 (d, 2H, J = 7.1 Hz), 3.64 (s, 3H), 3.41 (s, 2H), 2.81 (s, 4H), 2.32 (m, 4H), 2.09 (s, 3H), 1.61 (dd, 2H, J = 11.7, 5.9 Hz), 0.89 (t, 3H, J = 5.9 Hz). ^{13}C-NMR (101 MHz, DMSO-d6) δ 163.44, 155.83, 154.89, 146.45, 140.00, 128.99, 125.06, 117.69, 53.64, 49.06, 45.82, 45.27, 29.70, 22.71, 11.73. HRMS (ESI) calculated for $C_{20}H_{28}KN_8O_2S$ 483.1688, found 483.1695 [M+H]+

3.3.5.5 2-(3-(1-methylpiperazinesulfonylamino))-6-(isopropylamino)-9-methyl-9H-purine (18)

2-chloro-9-methyl-N-(2-methylpropyl)-9H-purin-6-amine 22c (1.0 eq) with 3-[4-methylpiperazin-1-yl)-sulfonyl] aniline 3a (1.2 eq), following the general synthetic

procedure E, the desired product 18 was obtained with 48.40% yield as a dark brown solid. 1H-NMR (500 MHz, DMSO-d6) δ 9.36 (s, 1H), 8.58 (s, 1H), 7.93 (s, 1H), 7.81 (s, 1H), 7.55 (s, 1H), 7.43 (t, 1H, J = 6.4 Hz), 7.13 (d, 1H, J = 6.5 Hz), 3.62 (s, 3H), 2.87 (s, 4H), 2.32 (s, 4H), 2.09 (s, 3H), 1.19 (t, 3H, J = 5.8 Hz), 0.89 (s, 3H), 0.87 (s, 3H). ^{13}C-NMR (101 MHz, DMSO-d6) δ 163.56, 142.66, 140.83, 139.81, 135.36, 129.90, 122.72, 119.40, 116.45, 53.57, 49.07, 45.86, 45.23, 36.54, 31.42, 20.38. HRMS (ESI) calculated for $C_{21}H_{31}N_8O_2S$ 459.2285, found 459.2276 [M+H]+

3.3.5.6 2-(4-(1-methylpiperazinesulfonylamino))-6-(isopropylamino)-9-methyl-9H-purine (19)

2-chloro-9-methyl-N-(2-methylpropyl)-9H-purin-6-amine 22c (1.0 eq.) and 4-[4-methylpiperazin-1-yl)-sulfonyl] aniline 3b (1.2 eq.), following the general synthetic procedure E, the desired product 19 was obtained with 72.03% yield as a dark brown solid. 1H-NMR (500 MHz, DMSO-d6) δ 9.56 (s, 1H), 8.08 (d, 2H, J = 7.1 Hz), 7.83 (s, 1H), 7.72 (s, 1H), 7.52 (d, 2H, J = 7.1 Hz), 3.64 (s, 3H), 2.81 (s, 4H), 2.31 (s, 4H), 2.09 (s, 3H), 1.19 (t, 2H, J = 5.8 Hz), 0.89 (s, 3H), 0.88 (s, 3H). ^{13}C-NMR (101 MHz, DMSO-d6) δ 155.89, 155.25, 146.81, 139.88, 128.99, 124.91, 117.62, 115.21, 54.06, 48.19, 46.27, 45.82, 29.80, 28.39, 20.75. HRMS (ESI) calculated for $C_{21}H_{30}KN_8O_2S$ 497.1844, found 497.1854 [M+H]+

3.3.5.7 2-(3-sulfonylamino)-6-(benzylamino)-9-methyl-9H-purine (20)

N-benzyl-2-chloro-9-methyl-9H-purin-6-amine 22a (1.0 eq.) and 3-aminobenzene sulfonamide (1.2 eq.), following the general synthetic procedure E, the desired product 20 was obtained with 33.42% yield as a yellow solid. 1H-NMR (500 MHz, DMSO-d6) δ 9.32 (s, 1H), 8.53 (s, 1H), 8.10 (s, 1H), 7.82 (s, 2H), 7.35 (s, 1H), 7.34 (s, 1H), 7.31 (t, 1H, J = 6.3 Hz), 7.25 (t, 3H, J = 6.0 Hz), 7.19 (s, 1H), 7.16 (t, 1H, J = 5.8 Hz), 4.69 (s, 2H), 3.63 (s, 3H). ^{13}C-NMR (101 MHz, DMSO-d6) δ 163.36, 156.22, 144.35, 142.26, 139.97, 129.51, 128.71, 127.60, 127.20, 121.49, 117.65, 115.34, 49.07, 29.63. HRMS (ESI) calculated for $C_{19}H_{20}N_7O_2S$ 410.1394, found 410.1409 [M+H]+

3.3.5.8 2-(4-sulfonylamino)-6-(benzylamino)-9-methyl-9H-purine (21)

N-benzyl-2-chloro-9-methyl-9H-purin-6-amine 22a (1.0 eq.) and 4-aminobenzene sulfonamide (1.2 eq.), following the general synthetic procedure E, the desired product 21

was obtained with 29.41% yield as a yellow solid. 1H-NMR (500 MHz, DMSO-d6) δ 9.41 (s, 1H), 8.24 (s, 1H), 7.85 (s, 1H), 7.81 (s, 1H), 7.55 (d, 2H, J = 6.7 Hz), 7.34 (d, 2H, J = 6.0 Hz), 7.28 (t, 2H, J = 6.1 Hz), 7.17 (t, 1H, J = 5.8 Hz), 7.08 (s, 2H), 4.69 (s, 2H), 3.64 (s, 3H). ^{13}C-NMR (101 MHz, DMSO-d6) δ 156.04, 154.91, 151.15, 145.27, 140.72, 140.08, 135.17, 128.75, 127.25, 127.12, 126.86, 117.48, 43.64, 29.81. HRMS (ESI) calculated for $C_{19}H_{20}N_7O_2S$ 410.1394, found 410.1406 [M+H]+

3.3.5.9 2-(3-(1-methylpiperazinesulfonylamino))-6-(benzylamino)-9-(oxan-2-yl)-9H-purine (33a)

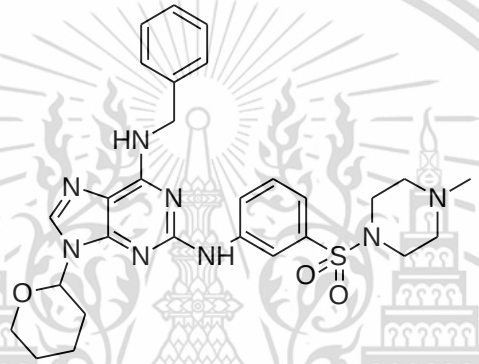

Compound 32a (1.0 eq.) and 3-[4-methylpiperazin-1-yl)-sulfonyl] aniline 3a (1.2 eq.), following the general synthetic procedure E, the desired compound 33a was obtained with 49.21% yield as a yellow solid. 1H-NMR (500 MHz, DMSO-d6) δ 9.44 (s. 1H), 8.68 (s, 1H), 8.22 (s, 1H), 8.08 (s, 1H), 7.79 (d, J = 5.1 Hz, 1H), 7.40 (t, J = 6.4 Hz, 1H), 7.32 (d, J = 5.9 Hz, 2H), 7.25 (t, J = 6.1 Hz, 2H), 7.16 (t, J = 5.8 Hz, 1H), 7.12 (d, J = 6.2 Hz, 1H), 5.50 (dt, J = 10.9, 5.5 Hz, 1H), 5.26 (s), 4.72 (s, 2H), 3.97 (t, J = 12.3 Hz, 1H), 3.64 (td, J = 9.1, 3.0 Hz, 1H), 2.78 (s, 4H), 2.24 (d, J = 13.2 Hz, 4H), 2.06 (s, 3H), 1.99 – 1.87 (m, 2H), 1.69 – 1.60 (m, 1H), 1.57 (dd, J = 11.8, 2.5 Hz, 2H), 1.19 (t, J = 5.8 Hz, 4H), 0.95 (t, J = 5.8 Hz), 0.81 (t, J = 5.5 Hz). MS-ESI: m/z 563.3 [M+H]+.

3.3.5.10 2-(3-sulfonylamino)-6-(isopropylpiperidin-4-amino)-9-(oxan-2-yl)-9H-purine (33b)

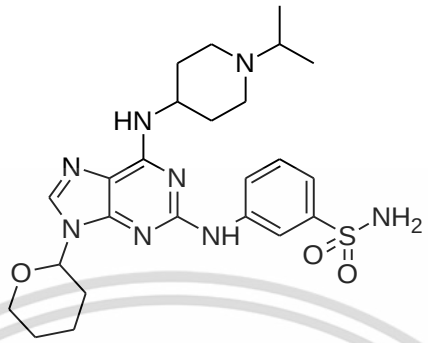

Compound 32b (1.0 eq.) and 3-aminobenzene sulfonamide (1.2 eq.), following the general synthetic procedure E, the desired compound 33b was obtained with 25.08% yield as a yellow solid. 1H-NMR (500 MHz, DMSO-d6) δ 9.30 (s, 1H), 8.70 (s, 1H), 8.04 (s, 1H), 7.75 (d, J = 5.6 Hz, 1H), 7.43 (d, J = 5.9 Hz, 1H), 7.36 (t, J = 6.3 Hz, 1H), 7.29 (d, J = 6.2 Hz, 1H), 7.20 (s, 1H), 5.53 (dd, J = 8.8, 1.1 Hz, 1H), 4.09 (dd, J = 8.4, 4.1 Hz, 1H), 3.99 – 3.94 (m, 1H), 3.66 (td, J = 9.1, 2.8 Hz, 1H), 2.74 (d, J = 8.7 Hz, 2H), 2.69 – 2.64 (m, 1H), 2.21 (d, J = 7.1 Hz, 4H), 1.94 (d, J = 9.6 Hz, 1H), 1.88 (d, J = 9.9 Hz, 1H), 1.79 (s, 2H), 1.72 – 1.63 (m, 1H), 1.57 – 1.51 (m, 4H), 0.95 (s, 3H), 0.93 (s, 3H). MS-ESI: m/z 515.2 [M+H]+.

3.3.5.11 2-(3-sulfonylamino)-6-(benzylpiperidin-4-amino)-9-(oxan-2-yl)-9H-purine (33c)

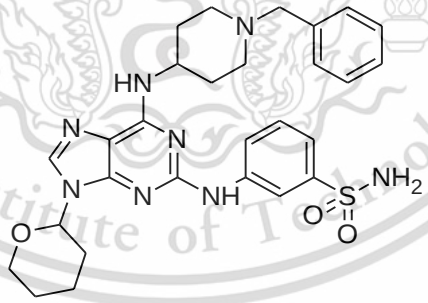

Compound 32c (1.0 eq.) and 3-aminobenzene sulfonamide (1.2 eq.), following the general synthetic procedure E, the desired compound 33c was obtained with 36.12% yield as a yellow solid. 1H-NMR (500 MHz, DMSO-d6) δ 9.31 (s, 1H), 8.68 (s, 1H), 8.04 (s, 1H), 7.77 (d, J = 5.6 Hz, 1H), 7.44 (d, J = 5.3 Hz, 1H), 7.36 (t, J = 6.3 Hz, 1H), 7.28 (t, J = 3.3 Hz, 4H), 7.21 (dt, J = 4.1, 2.0 Hz, 3H), 4.12 (s, 1H), 3.96 (d, J = 9.0 Hz, 1H), 3.67 (td, J = 9.2, 2.6 Hz, 1H), 3.45 (s, 2H), 2.78 (d, J = 8.9 Hz, 2H), 2.19 (d, J = 8.8 Hz, 1H), 2.07 (t, J = 8.7 Hz, 2H),

1.94 (d, J = 9.8 Hz, 1H), 1.88 (d, J = 8.3 Hz, 2H), 1.79 (s, 2H), 1.62 (dd, J = 19.9, 9.7 Hz, 4H), 1.53 (s, 2H). MS-ESI: m/z 563.4 [M+H]+.

3.3.6 General synthesis procedure F

A mixture of product which received from general synthetic procedure E (1.0 eq) in anhydrous DCM and TFA = 50/50 total 5 ml was stirred at room temperature for 5 h. until its completion. The reaction mixture was extracted with 10% $NaHCO_3$ in water and DCM (3 x 10 ml), the organic phases were combined, dried over anhydrous Na_2SO_4 and concentrated under reduced pressure to with no purification to afford the desired product as a yellow solid. However, this reaction will generate tautomerized conformation according to the report of coexisting tautomers of purine bases39-40, with the prototropic 7H and 9H as the desired species, where the intramolecular proton-transfer is accompanied by migration of **π** electrons. Generally, their relative populations could be affected by structural factors such as aromaticity, intramolecular interactions, substituent effects able to modify the electronic distribution within the molecule, repulsions of lone electron pairs. Additionally, external influences are also the cause such as solvent and temperature.

3.3.6.1 2-(3-(1-methylpiperazinesulfonylamino))-6-(benzylamino) purine (23)

2-(3-(1-methylpiperazinesulfonylamino))-6-(benzylamino)-9-(oxan-2-yl)-9H-purine 33a was proceeded, following the general synthetic procedure F, the desired product 23 was obtained as a yellow solid with 78.39% yield. 1H-NMR (500 MHz, DMSO-d6) δ 9.30 (s, 1H), 8.42 (s), 8.06 (s, 1H), 7.92 (s, 1H), 7.85 (s, 1H), 7.40 (t, 1H, J = 6.4 Hz), 7.35 (s, 1H), 7.33 (s, 1H), 7.26 (t, 2H, J = 6.1 Hz), 7.17 (t, 1H, J = 5.8 Hz), 7.12 (d, 1H, J = 6.2 Hz), 4.73 (s, 2H), 2.89 (s, 4H), 2.65 (s, 4H), 2.33 (s, 3H). HRMS (ESI) calculated for $C_{23}H_{27}N_8O_2S$ 479.1972, found 479.2010 [M+H]+

3.3.6.2 2-(3-sulfonylamino)-6-(isopropylpiperidin-4-amino) purine (35)

2-(3-sulfonylamino)-6-(isopropylpiperidin-4-amino)-9-(oxan-2-yl)-9H-purine 33b was proceeded, following the general synthetic procedure F, the desired product 35 was obtained as a yellow solid with 17.53% yield. 1H-NMR (500 MHz, DMSO-d6) δ 9.39 (s, 1H), 9.20 (s, 1H), 8.91 (s, 1H), 7.98 (s, 1H), 7.91 (s, 1H), 7.50 (s, 1H), 7.42 (t, J = 7.8 Hz, 1H), 7.37

– 7.29 (m, 3H), 4.48 (s, 1H), 3.24 (t, 4H), 2.18 (d, J = 10.1 Hz, 2H), 1.98 – 1.88 (m, 2H), 1.30 (d, J = 6.6 Hz, 6H). ^{13}C-NMR (101 MHz, DMSO-d6) δ 156.15, 153.54, 144.62, 142.58, 129.39, 121.39, 117.51, 114.80, 57.61, 47.35, 45.57, 29.58, 16.87. HRMS (ESI) calculated for $C_{19}H_{27}N_8O_2S$ 431.1972, found 431.1961 [M+H]+

3.3.6.3 2-(3-sulfonylamino)-6-(benzylpiperidin-4-amino) purine (36)

2-(3-sulfonylamino)-6-(benzylpiperidin-4-amino)-9-(oxan-2-yl)-9H-purine 33c was proceeded, following the general synthetic procedure F, the desired product 36 was obtained as a yellow solid with 14.94% yield. 1H-NMR (500 MHz, DMSO-d6) δ 12.48 (s, 1H), 9.20 (s, 1H), 8.41 (s, 1H), 7.93 (s, 1H), 7.84 (s, 1H), 7.40 – 7.31 (m, 4H), 7.28 (s, 1H), 4.22 (s, 1H), 3.71 (s, 2H), 2.97 (s, 2H), 1.94 (s, 2H), 1.74 (s, 2H). ^{13}C-NMR (101 MHz, DMSO-d6) δ 156.25, 154.13, 144.70, 142.69, 137.08, 129.59, 128.80, 128.04, 121.24, 117.37, 115.17, 70.23, 52.13, 46.07, 29.45. HRMS (ESI) calculated for $C_{23}H_{27}N_8O_2S$ 479.1972, found 479.1956 [M+H]+

3.4 Phosphodiesterase Inhibition

PDE5 and PDE1 activity were assessed using a protocol previously reported elsewhere.[61] Human PDE5 plasmid, obtained as a gift from Professor Dr Joseph A. Beavo, University of Washington, Seattle, WA, USA, were sub-cloned into a pcDNA3 vector containing an ampicillin resistant gene.[62] Bovine heart PDE1 was purchased from Sigma-Aldrich. Briefly, a reaction mixture comprising 25 µL of 10 mM EGTA, 25 µL of buffer C (100 mM Tris–HCl (pH 7.5), 100 mM imidazole, 15 mM $MgCl_2$ and 1.0 mg/ml BSA), 25 µL of PDE solution, 25 µL of test sample or solvent (5% DMSO) only as a control. The reaction was started by adding substrate 25 µL of 1 µM [3H] cGMP (~50,000 cpm) and the solution was incubated at 30 ºC for 10 min. The reaction was stopped by placing the tube in boiling water for 1 min and then cool. In the next step, 25 µL of snake venom were added and the solution was incubated at 30°C for 5 min. The assay was diluted with 250 µL of low salt buffer (20 mM Tris–HCl, pH 6.8) and transfer to a DEAE ion exchange resin column. The [3H] guanosine was eluted from resin with 1000 µL of low salt buffer, two times and the eluates were collected in a scintillation vial. Four mL of the scintillant cocktail were

added to the vial and mixed completely. The radioactivity of the cocktail was measured by using a liquid scintillation counter (Tri-Carb 2910 TR; Perkin Elmer). In the case of the PDE1 inhibitory activity assay, EDTA was used instead of EGTA, and 4 mM $CaCl_2$ and 16 µg/mL calmodulin were added to buffer C. The PDE enzymes in the study were standardized to have a hydrolysis activity of 20–30% of the total substrate counts.

All samples were dissolved in DMSO and diluted with water. DMSO was limited to 1% in the final assay medium. In preliminary screening, pure compounds tested at 10 µM final conc for triplicate. When PDE inhibition was >80%, samples were re-analyzed to find IC_{50}s. IC_{50}s were calculated from 8 activities at different concentrations ranging from 50-0.0001 µM. IC_{50}s were calculated using Prism software (Graph Pad Inc., San Diego, CA). Sildenafil was used as the positive control.

3.5 Aqueous Solubility

The equilibrium solubility was determined in phosphate buffer (PBS) at $pH_{7.4}$.[63] Approximately 1 mg of each sample was soluble in 2 mL of 0.02 M PBS at $pH_{7.4}$ in a 10 mL glass screw top vial, sonicated and shaken for 1 hr and 6 hrs, respectively, to make the saturated solution, and then filtered using a syringe filter (13mm, 0.20 µm, filter, Xiboshi). A standard solution of each sample was prepared by dissolving a known amount of sample in 1 mL of DMSO, pre-diluted by 10-times using DMSO. The amount of sample present in the PBS and DMSO solutions was determined by HPLC-UV (HITACHI/Chromaster HPLC with a SunShell 2.6 C8, 2.6 µM column). A 100 µL injection of the aqueous sample and 10 µL of DMSO solution were used. The solubility was calculated based on the ratio of the area under the curve obtained from the 2 samples, corrected for the dilution factors and injection volume.

3.6 Partition coefficient ($logD_{7.4}$)

Compounds were dissolved in 1-octanol, pre-saturated with 0.02M PBS at $pH_{7.4}$ and evaluated using the shake flask technique[64]. Roughly 1 mg of the sample was added into a 10 mL glass screw-top vial to which 2 mL of octanol was added. The solution was

sonicated for 1 hr. Compounds that incompletely dissolved were diluted in further octanol and sonicated until a completely clear solution resulted. A final volume of 2mL of octanol solution and 8 mL of 0.02 M of PBS at $pH_{7.4}$ were shaken for 6 hrs. The resulting solutions were centrifuged (4000 rpm for 15 min), and the octanol and aqueous layers were extracted separately. The amount of sample present in the octanol and PBS solutions were determined by HPLC-UV (HITACHI/Chromaster HPLC with a SunShell 2.6 C8, 2.6 µM column). An injection volume of 100 µL of the aqueous sample and 10 µL of the octanol solution (pre-diluted 10-times using DMSO) were used. The $logD_{7.4}$ value was calculated from the area under the curve obtained from the 2 phases, corrected for the dilution factors and injection volume as well as the aqueous solubility test.

Chapter 4
Result and Discussion

4.1 Binding Mode Assessment

The determination of the binding mode of our most promising lead from earlier research, **A**[13, 15] was initial goal of the research project. Conformational analysis of the molecule was undertaken by the rotating the amine groups attached the 2 & 4-position of quinazoline relative to each other. Quantum mechanical optimization at the HF/6-31G(d) level of theory was then undertaken. Four distinct minima were obtained, labelled hence forth conf-1 to conf-4 (Figure 2). Conf-2 and conf-4 were approximately isoenergetic and considerably lower in energy than conf-1 and conf-2. This was due to reduced steric interaction between the quinazoline ring and the 4-position substituent. The sizeable energy difference, and the sub-μM potency suggests that the inhibitor should only bind to PDE5 in one of these two conformations.

4.2 Ligan-based methods

A ligand-based approach can be used to assess the most likely binding mode of a molecule by overlaying it to the active conformation of known inhibitors extracted from experimental x-ray structures. We assess the 3D similarity of **A** to the active PDE5 inhibitor conformations of Vardenafil (1XP0[42]), Sildenafil (1UDT[43]), Tadalafil (1XOZ[42]), and Avanafil (6L6E[44]). The shape and pharmacophore similarity of the conf-1-conf4 were evaluated using ShaEP[45] and PharmaGist[46, 47], respectively (Figure 2). Shape-based analysis pointed to conf-2 and conf-4 showed the highest average shape similarity across all 4 inhibitor references. Conf-2 displayed the highest score at 0.540, closely followed by conf-4 at 0.538. Both conformations showed the highest similarity to the reference Tadalfil. Pharmacophore analysis identified that conf-4 was the highest scoring of all conformations, while conf-2 was the lowest scoring of the four. All conformations showed the highest similarity to Sildenafil. It was noted that despite identifying the lowest energy conformations as having greater overlap with the inhibitor queries, when viewed in the

context of the protein, these overlays often clashed with amino acid residues. This prompted us to consider a structure-based approach

4.3 Structure-based method

The four QM optimized conformations of **A** were used as input for docking to PDE5. Docking to multiple X-ray structures was investigated due to subtle differences each inhibitor can have on the active site cavity[65]; Vardenafil (1XP0[42]), Sildenafil (1UDT[43]), Tadalafil (1XOZ[42]), and Avanafil (6L6E[44]). Protein preparation prior to docking involved removing the bound inhibitors, water molecules and other cofactors. In addition, a docking constraint was imposed requiring each ligand pose to have a H-bond interaction with Gln817. Three distinct poses were found from the docking exercise and all poses were found to adopt confirmation equivalent to low energy conformations 2 and 4 (Figure 2). Pose-1 was generated in only 2 protein structures (1XP0 & 6L6E). The inhibitor makes a single H-bond to Gln817 and forms **π** stacking interactions with Phe786 and Phe820 and His613. Inhibitor conf-4 was observed for the binding pose. Binding pose-2 was generated in 3 X-ray structures, displays two H-bonds with Gln817 and **π** stacking with Phe-786 and Phe820 and His613. Inhibitor conf-2 was observed for the binding pose. Binding pose-3 was also found in 3 X-ray structures, has a single H-bond with Gln817 and **π** stacking with Phe786 and Phe820 is observed. Inhibitor conf-4 was also observed for the binding pose. It was noted that docking poses to 1X0Z could be generated due to the buried nature of Gln817. Furthermore, molecular docking scores were not relied upon to rank order the docked poses as it is known that these can be unreliable. Warren et al noted that the experimental binding pose was typically observed within the top 3 docking poses across a diverse target set.[66] The docking poses were rank-ordered from an analysis of data generated from 5 ns molecular dynamics simulations of the corresponding protein-inhibitor complexes.

Table 1. Key MD parameters obtained from the simulation of 3-poses of **A** docked to PDE5 structure 1XP0.[42] Distances in Å. Standard deviations are noted in parentheses.

PDE5 Binding	Pose-1	Pose-2	Pose-3
Conformation	conf-4	conf-2	conf-4
Docking Score	71.44	62.78	75.15
RMSD protein	0.198 (0.010)	0.183 (0.009)	0.197 (0.010)
RMSD ligand	0.196 (0.032)	0.195 (0.030)	0.183 (0.030)
Gln817 NH_2 or HB1 distance	5.893 (0.231)	1.881 (0.112)	3.826 (0.276)
Gln817 C=O or HB2 distance	2.241 (0.234)	2.182 (0.210)	4.444 (0.357)

The relative stability of the complexes can be assessed in terms of the protein and ligand conformational fluctuation/deviation (RMSD), while an assessment of the inhibitor binding strength could be inferred from the average H-bond interaction distance. Simulations were performed in Gromacs 2019.4[49, 67] using the General force field/GAFF (AMBER96SB).[38] Parameters extracted from the simulations are illustrated in Figure 8 and Table 1. Pose-2 results in a considerably smaller deviation in the protein conformation, and fluctuates less significantly, over the course of the 5ns simulations than the other two conformations (0.18 vs 0.20 Å). The strength of interaction between the ligand and protein can be assessed from both the RMSD and the H-bond distances. Pose-3 displays the lowest ligand RMSD, however the mean H-bond distances made with Gln817 are ~4 Å indicating no H-bond is formed with this key residue. Pose-2 maintains its two strong H-bond interactions with Gln817, at 1.9 and 2.2 Å, respectively. Pose-1 makes a single strong H-bond interaction, at 2.2 Å on average. It was concluded that pose-2 is the most probable binding mode of **A** to PDE5. Firstly, the molecule binds in conf-2, 1 of the 2 low energy QM ligand conformations, results in the most stable protein-ligand complex from MD, and makes 2 H-bond interactions with Gln817, consistent with 75% of known inhibitors that make a bidentate, rather than monodentate interaction. Furthermore, the ligand conf-2

was also found to be 1 of the 2 conformations with highest shape similarity to 4 known PDE5 inhibitor reference conformations that were taken from PDB structures.

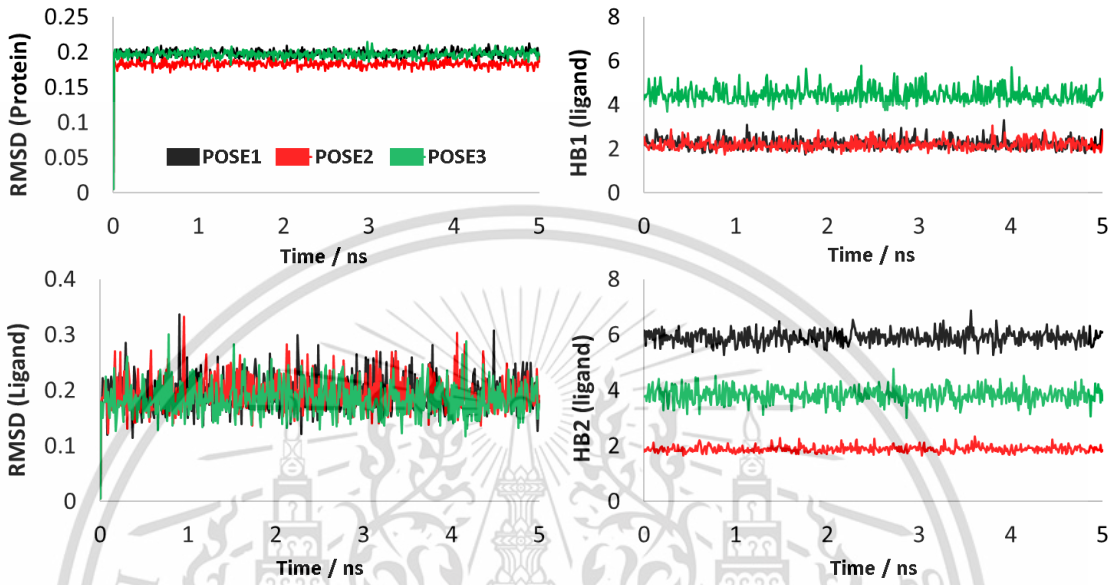

Figure 7. MD parameters of different binding modes of **A** to PDE5 in different ways (pdb code: 1UDT[43]). (A) Pose-1 has one H-bond interaction with Gln817 while (B) Pose-2 formed two H-bond with Gln817, (C) Pose-3 makes one weak interaction between $SONH_2$ group with Gln817. Distances plotted in nm

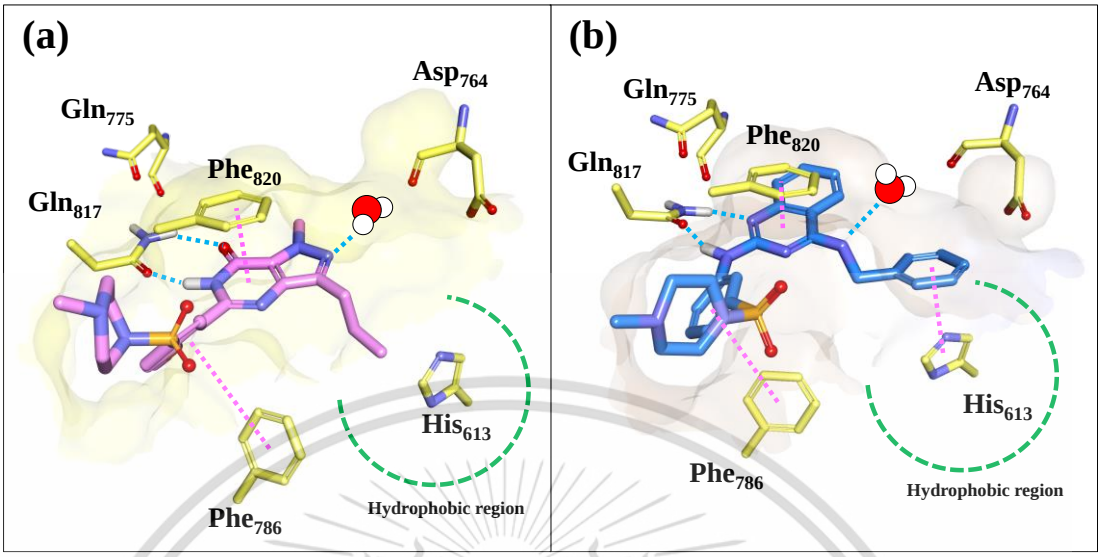

Figure 8. (a) Experimental binding mode of Sildenafil to PDE5[43] compared to the predicted docking of **4** consistent with pose-2. Key active site residues and interactions are shown (H-bond=blue, **π**-stacking=pink).

4.4 Structure-based design

The structure-guided design of new compounds was undertaken based on the predicted binding mode described by pose-2 (Figure 7). Synthetic modifications to were developed, consisting of alterations to the scaffold and changes to the steric and electronic characteristics to the amines incorporated at the 2 & 4 positions of quinazoline. The modifications were; (1) We investigated the capping of the anilinosulfonamide of the lead compound with methylpiperizine. Based on the molecular docking, this would put the piperazine ring in position analogous to that occupied by the same group based on Sildenafil and Vardenafil X-ray structures (Figure 7). The resulting increased interaction with solvent would help to maximize solubility due to presence of basic center, while an activity increase due to increased Van der Waals contacts with the protein might also be expected. The binding mode adopted with the inclusion of 3-(piperazine-1-sulfonyl) aniline (**4**) is shown in Figure 8. (2) Exchange of the 4-position aromatics with various aliphatic groups was next considered. While **π**-stacking with His613 is possible if the residue is protonated state, modification to a smaller aliphatic substituent would lower the lipophilicity. This modification is also consistent with Sildenafil, which as a propyl

substitent in the equivalent pocket (Figure 7). (3) An alternative modification to quinazoline 4-position was the replacement of the aromatic benzyl groups with a basic piperidin-4-amines which could potentially interact with Asp764. The swapping of a **π**-interaction for a salt bridge could potentially result in both improved solubility and PDE5 activity. (4) Introduction of methoxy substituents at the 6,7 positions of quinazoline were also investigated to explore non-polar interactions within this pocket. In addition, the opportunity exists to displace active site bound water molecules thereby improving the entropic contribution to the binding energy. (5) Scaffold hopping from quinazoline to the more polar purine core was also considered. Incorporation of a hydrophobic methyl group at the purine 9-position, more closely mimicking quinazoline, or with hydrogen was investigated. Both are more polar alternatives, with the latter offering the possibility of interaction with the side chain of Gln775. Finally, 5 analogs were prepared incorporating a combination of a basic center with methoxy substituents or a basic center with a purine scaffold.

Table 2. Inhibitory activity of compounds **4-36** against PDE5. Also reported are the overall yields, molecular weight, and calculated lipophilicities.

ID	R^1	R^2	R^3	Overall Yield	%Inhibition PDE5 (1 μM)	PDE5 IC_{50} (μM)	clogP[a]	$clogD_{7.4}$[a]	MWT[a]
A		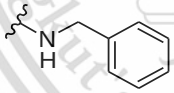	3-SO_2NH_2	66.5	100.53±2.85	0.10±0.01	3.94	3.94	405.48
4		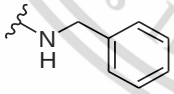	3-SO_2-methyl piperazine	40.9	98.29±1.13	0.50±0.18	4.24	4.22	488.61
5		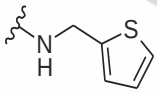	3-SO_2-methyl piperazine	45.2	93.91±1.63	0.52±0.30	4.15	4.13	494.63
6		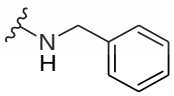	4-SO_2-methyl piperazine	26.6	96.47±0.38	0.49±0.18	4.24	4.22	488.61
7		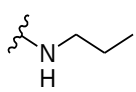	3-SO_2-methyl piperazine	32.0	96.90±0.57	0.60±0.21	3.39	3.37	440.57
8		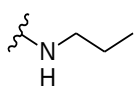	4-SO_2-methyl piperazine	3.0	95.57±3.23	0.41±0.17	3.39	3.37	440.57

9		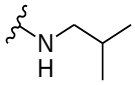	3-SO_2-methyl piperazine	8.6	97.31±2.03	0.43±0.30	3.76	3.74	454.59
10		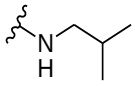	4-SO_2-methyl piperazine	5.7	98.97±2.72	0.36±0.24	3.76	3.74	454.59
11	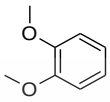	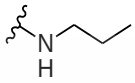	3-SO_2NH_2	66.5	91.64±2.83	1.44±0.11	2.78	2.78	417.48
12	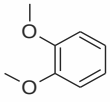	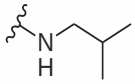	3-SO_2NH_2	48.2	94.91±2.11	5.23±4.63	3.15	3.14	431.51
13	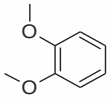	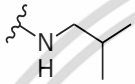	4-SO_2NH_2	37.1	94.58±2.69	3.97±0.32	3.15	3.14	431.51
14	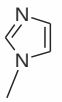	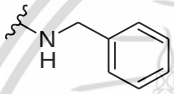	3-SO_2-methyl piperazine	41.4	69.01±5.64	nd	2.74	2.72	492.6
15	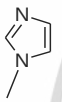	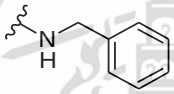	4-SO_2-methyl piperazine	17.7	97.33±3.17	38.37±11.21	2.74	2.72	492.6
16	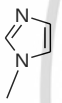	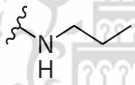	3-SO_2-methyl piperazine	11.8	93.57±4.47	43.16±14.42	1.89	1.87	444.56
17	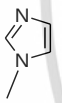	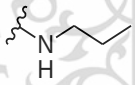	4-SO_2-methyl piperazine	11.5	93.61±2.01	18.88±3.66	1.89	1.87	444.56
18	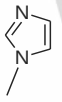	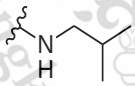	3-SO_2-methyl piperazine	15.8	91.80±3.65	33.26±3.83	2.26	2.24	458.59
19	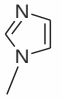	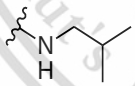	4-SO_2-methyl piperazine	18.5	95.96±1.92	28.54±0.98	2.26	2.24	458.59
20	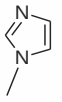	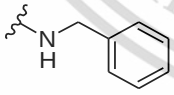	3-SO_2NH_2	31.0	86.10±1.72	4.46±1.92	2.44	2.44	409.42
21	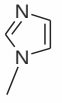	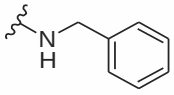	4-SO_2NH_2	27.3	96.53±0.82	23.01±3.86	2.44	2.44	409.42
23	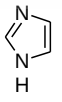	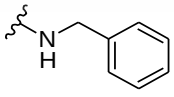	3-SO_2-methyl piperazine	23.6	99.26±2.01	2.02±0.38	2.51	2.47	478.58
24		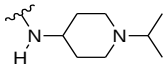	3-SO_2NH_2	48.9	96.34±0.96	1.03±0.11	2.77	1.12	440.57

25		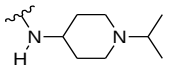	3-SO_2-methyl piperazine	39.0	93.56±1.90	0.15±0.02	3.31	1.40	523.70
26		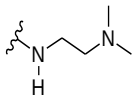	3-SO_2NH_2	53.0	72.16±6.44	9.39±2.54	2.02	0.86	386.47
27		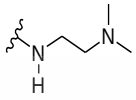	3-SO_2-methyl piperazine	19.6	75.35±1.94	5.28±0.84	2.53	1.13	469.61
28		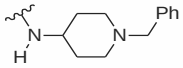	3-SO_2NH_2	19.9	93.44±1.96	0.22±0.01	3.77	2.65	488.61
29	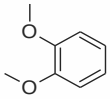	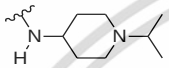	3-SO_2NH_2	56.1	79.32±1.88	3.41±0.60	2.45	0.79	500.62
30	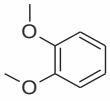	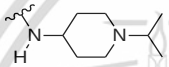	3-SO_2-methyl piperazine	15.1	18.53±7.69	nd	3.00	1.07	583.75
34	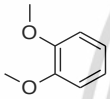	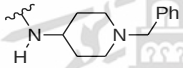	3-SO_2NH_2	78.7	93.69±2.67	1.64±0.22	3.45	2.32	548.66
35		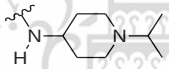	3-SO_2NH_2	3.4	32.66±6.51	nd	0.76	-0.56	430.53
36		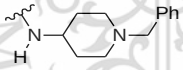	3-SO_2NH_2	3.5	94.34±0.33	0.29±0.01	1.99	0.96	478.58
Sildenafil				-	-	0.0014±0.0002	1.35	1.32	474.58

4.5 Synthesis

All compounds were prepared according to synthetic routes described in Scheme 1. For example, **4** was produced by the substitution of benzylamine at the 4-position 2,4 dichloroquinazoline with assistance of TEA for 6-8 hrs at room temperature to give intermediate **1b,** in a yield of 52.7%. Intermediate **2a** was prepared from reaction of 3-nitrobenzenesulfonylchloride and 1-methyl piperazine with TEA as basic catalyst, from 0°C to room temperature, for 2 hrs, in a yield of 82.6 %. The amine product was hydrogenated using H_2, Pd/C in methanol at room temperature for 2 hrs giving **3a** in a yield of 95.5 %. **1b** was then reacted with **3a** assisted by 1M HCl in iso-propyl alcohol at 90° for 8 hrs giving compound **4** in a yield of 92.5 %. The overall yield of from 4 steps was 40.9 %.

Intermediates **2b** and **3b** were synthesized following the same procedure as **2a** and **3a**, in yields of 91.8 % and 67.8 %, respectively. Compound **5-13, 24-30** and **34** were synthesized by using the same protocol as **4**. Overall yields ranged from 3.0-78.7 %. Purine analogs such as compound **14** were produced by coupling 2,6-dichloro-9-methyl-9h-purine and benzylamine using DIPEA in n-butanol at 90℃ for 6 hrs to get intermediate **22a** with a yield of 92.7 %. **22a** was substituted by **3a** at the 2-position using $Pd_2(dba)_3$, Xphos and K_2CO_3, in anhydrous dioxane at 110 ℃ under a nitrogen environment, overnight, to give **14** with a yield of 56.7 %. Compounds **15-21** were synthesized following the same route**.** Compound **23,** having a H atom at 9-position of purine, required an additional protection step.[68] 2,6-dichloro-9H-purine was reacted with DHP in ethyl acetate with para-toluene sulfonic acid in EtOAc at room temperature for 5 hrs, giving **31a**. Substitution at the 6-position of **31a** was achieved using analogous conditions as used for the 4-positon of quinazoline. Substitutions at the 6-position of **31a** followed the same conditions as those used for the 4-position of quinazolines, giving **32a** in 85.4 % yield. Substition of the 2-position of **32a** followed the same conditions as those used for the 4-position of quinazolines, giving **33a** in 49.2 % yield. Deprotection of **33a**, was performed using concentrated TFA in dichloromethane at room temperature for 3 hrs, giving **23** in 78.4 % yield. Twenty-nine novel compounds were synthesized in total according to Scheme 1 with overall reaction yields ranging from very low (3.0 %), for 9*H*-purines, to excellent (78.7 %), for quinazolines lacking a basic center.

4.5.1 The characterization data for compound 8, 9, 10, 25, and 36

The ^{1}H-NMR, ^{13}C-NMR, MS, HPLC UV data for the most potent exemplars are shown in Figure 9-Figure 28 for the purpose of illustration

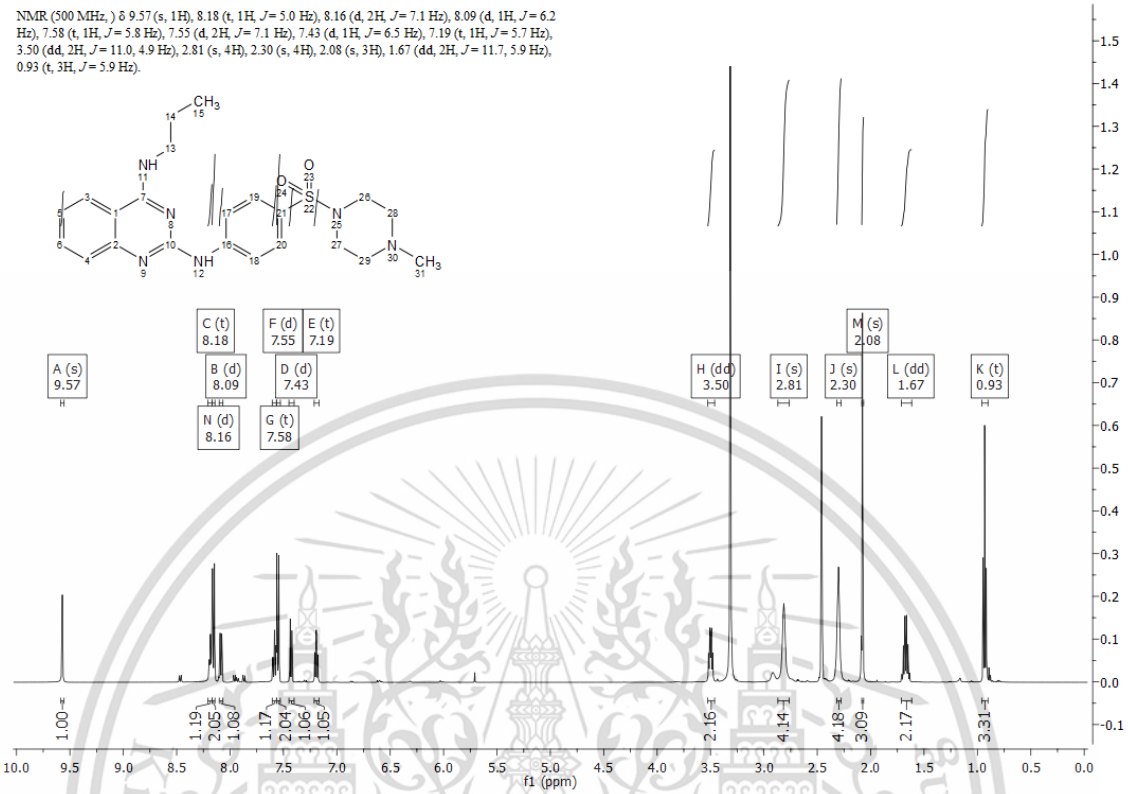

Figure 9. ^{1}H-NMR spectra of compound 8

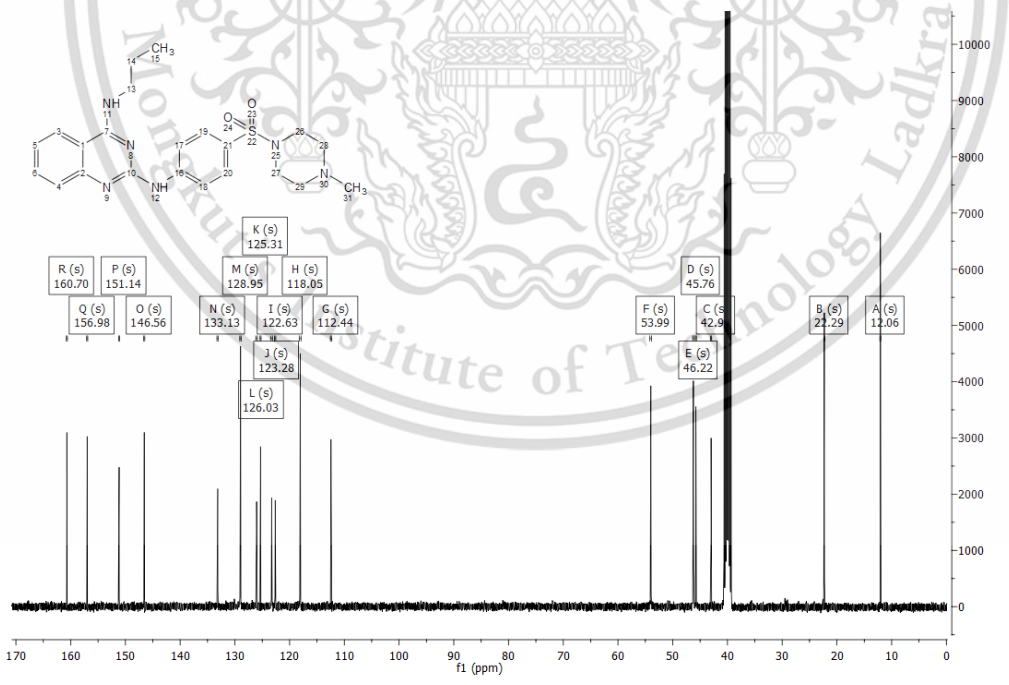

Figure 10. ^{13}C-NMR spectra of compound 8

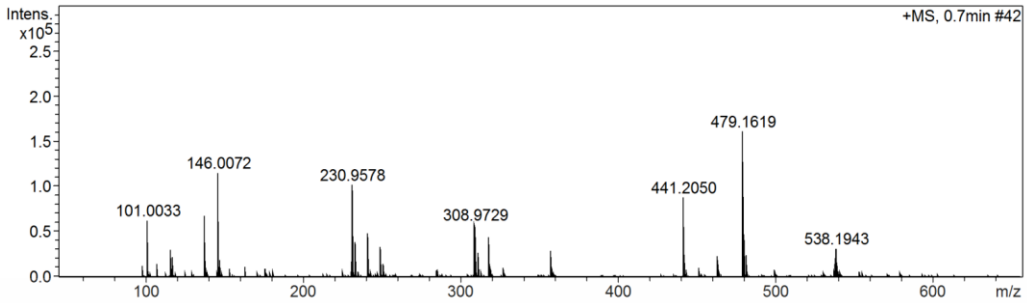

Figure 11. HRMS spectra of compound 8

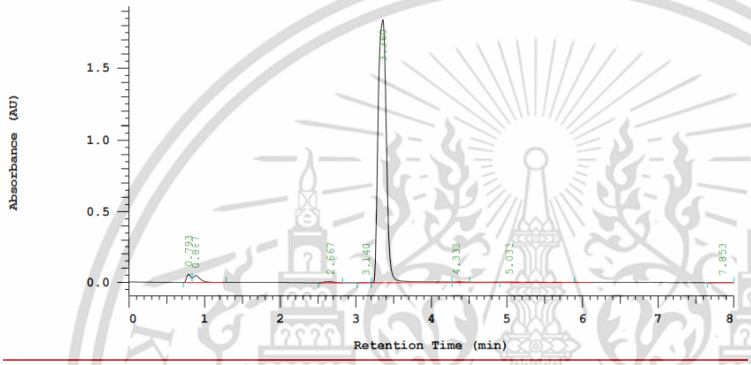

Figure 12. HPLC spectra of compound 8

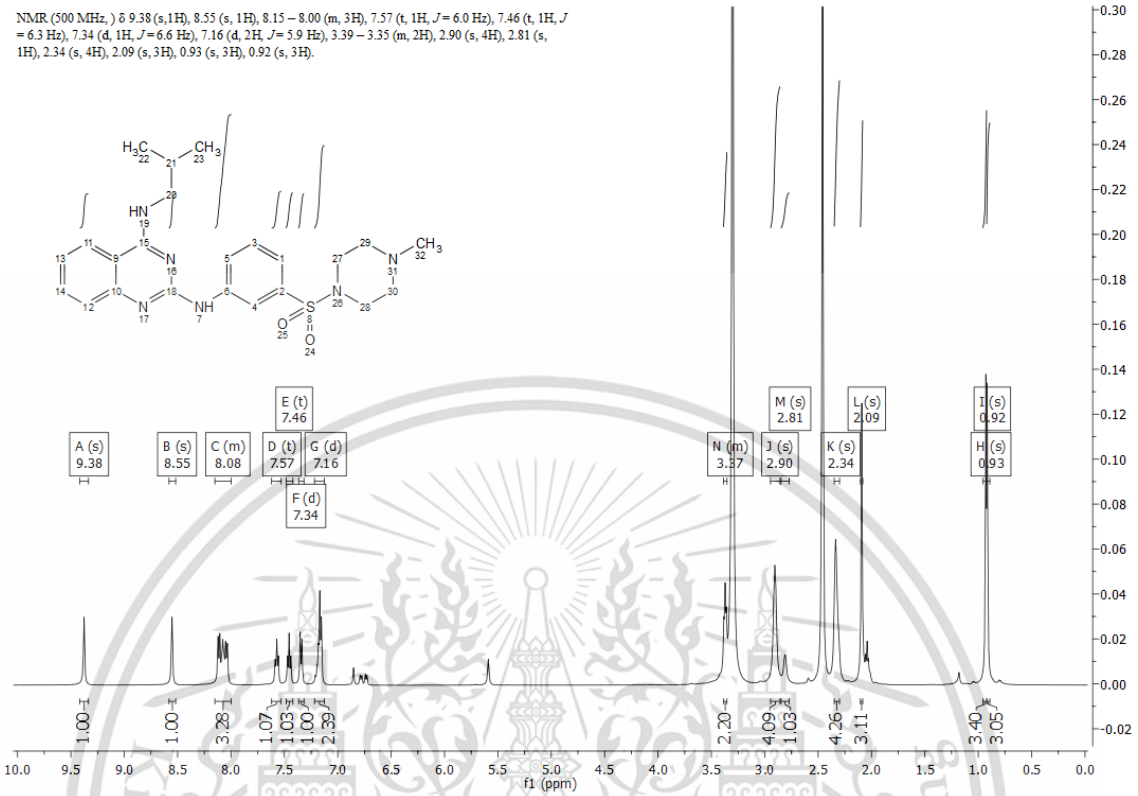

Figure 13. ^{1}H-NMR spectra of compound 9

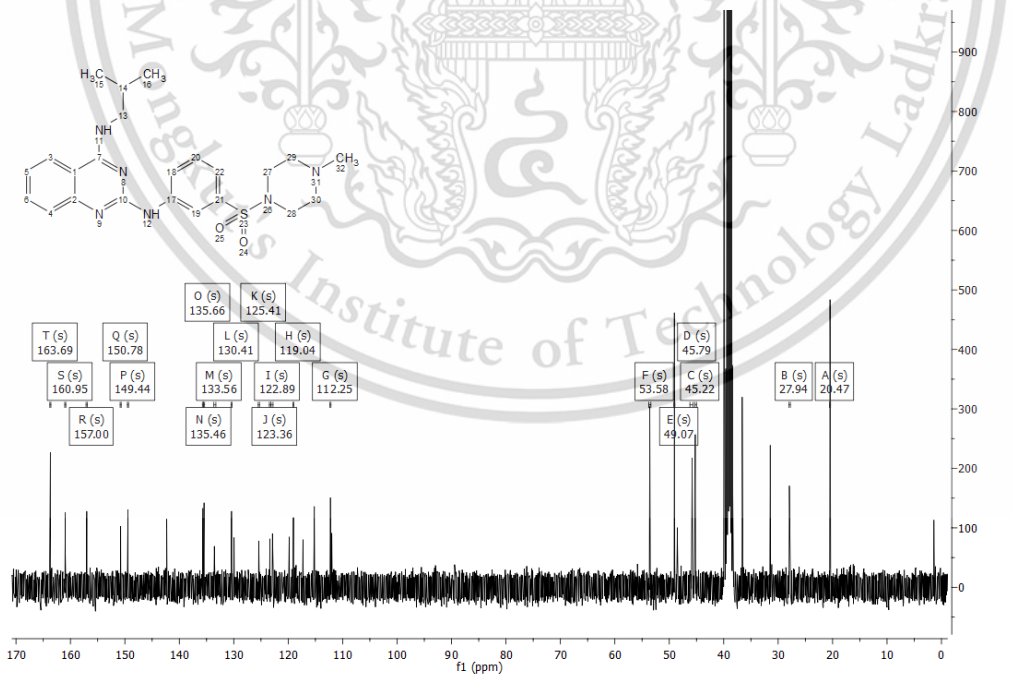

Figure 14. ^{13}C-NMR spectra of compound 9

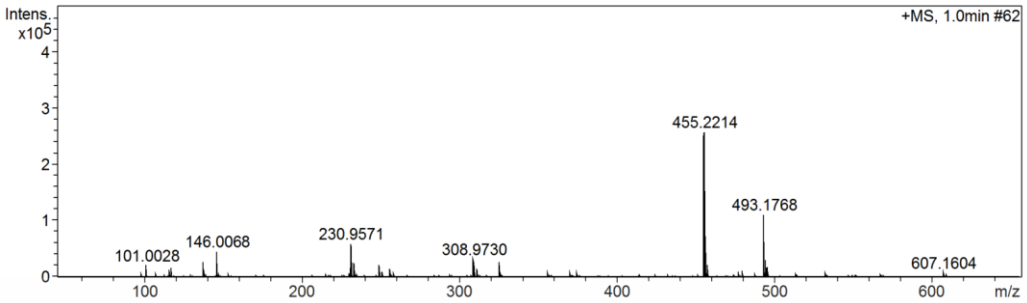

Figure 15. HRMS spectra of compound 9

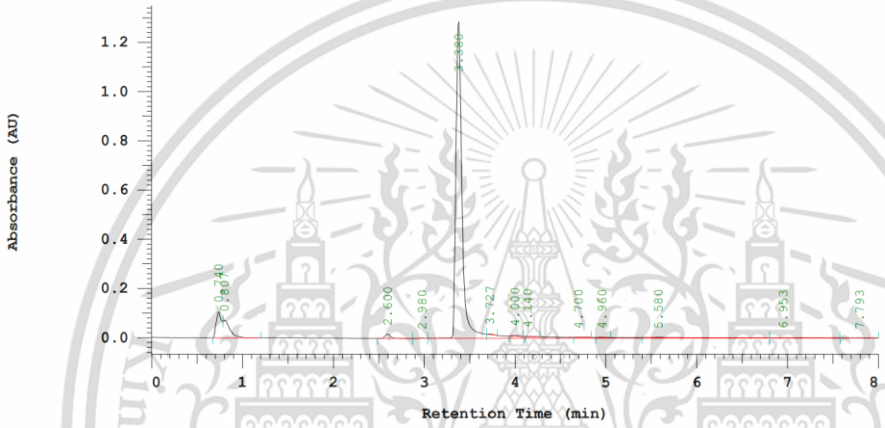

Figure 16. HPLC spectra of compound 9

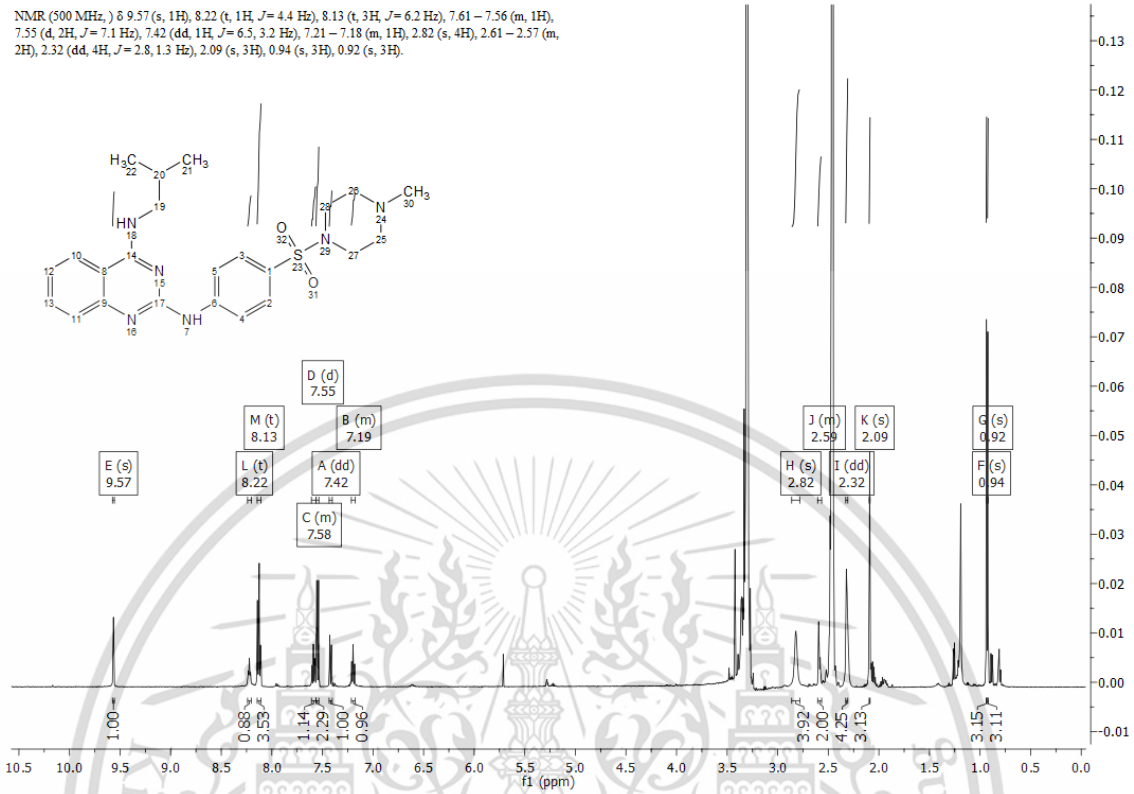

Figure 17. ^{1}H-NMR spectra of compound 10

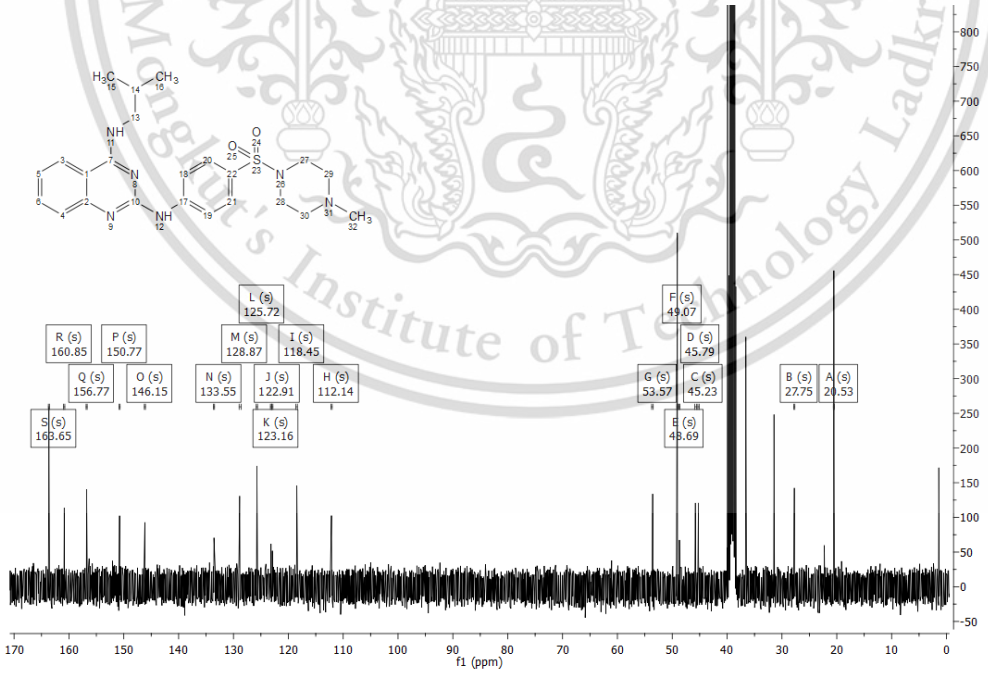

Figure 18. ^{13}C-NMR spectra of compound 10

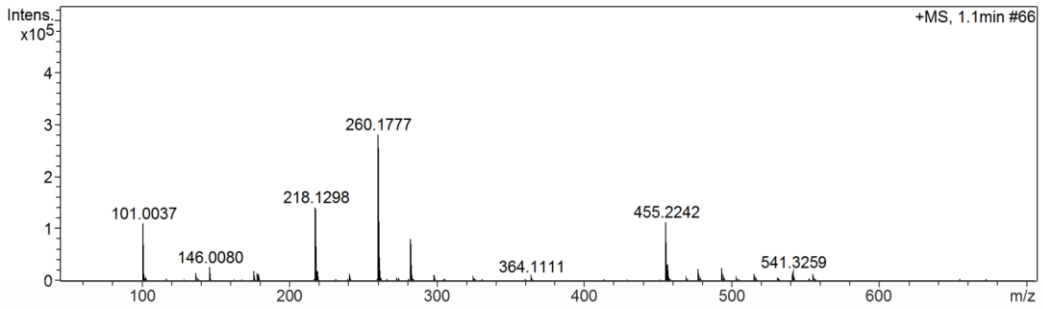

Figure 19. HRMS spectra of compound 10

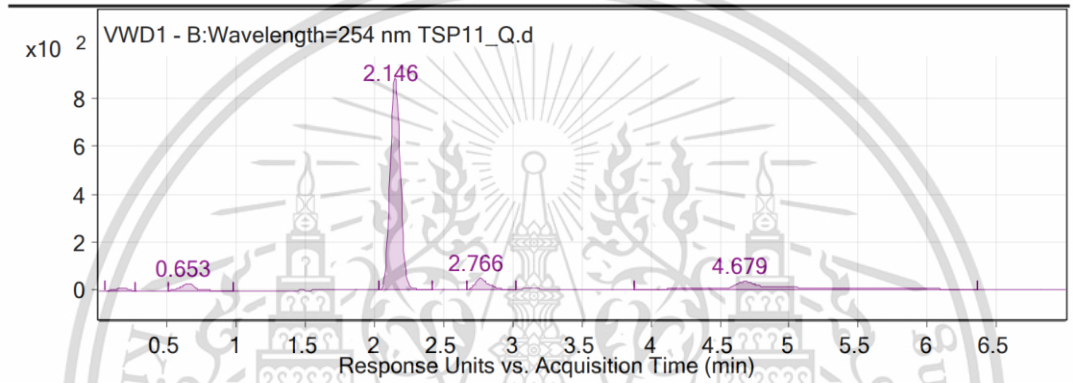

Figure 20. HPLC spectra of compound 10

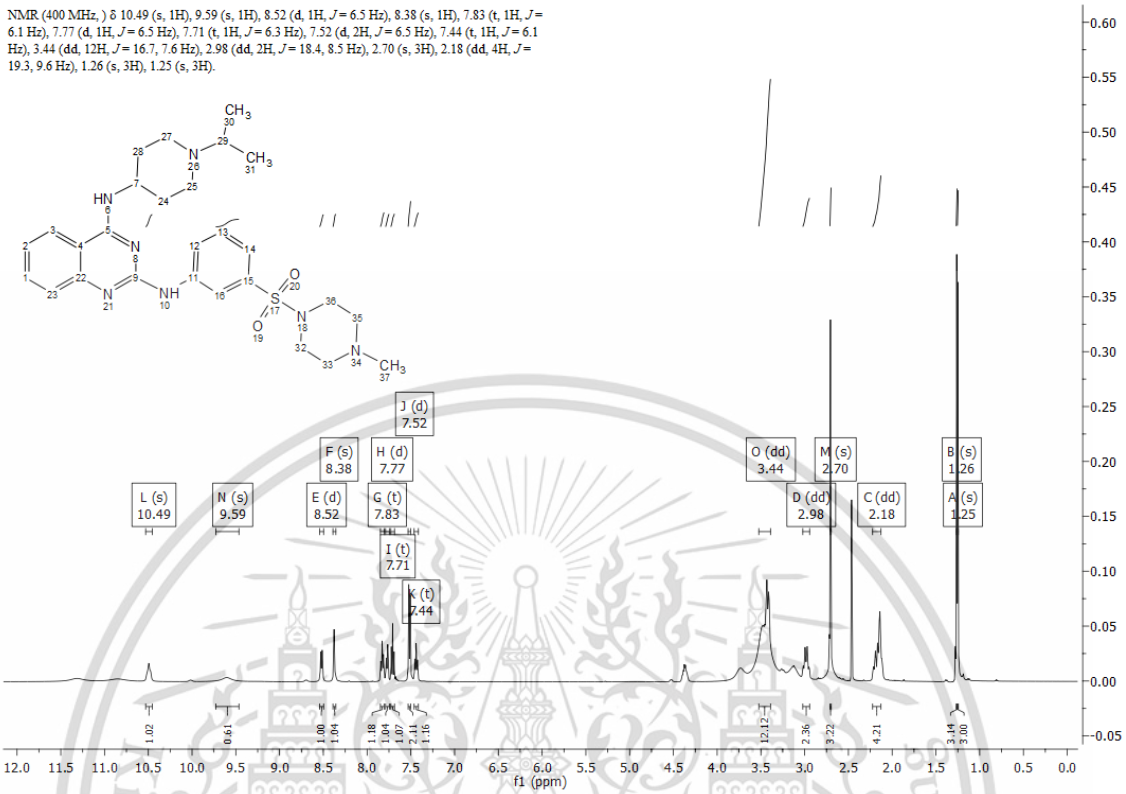

Figure 21. ^{1}H-NMR spectra of compound 25

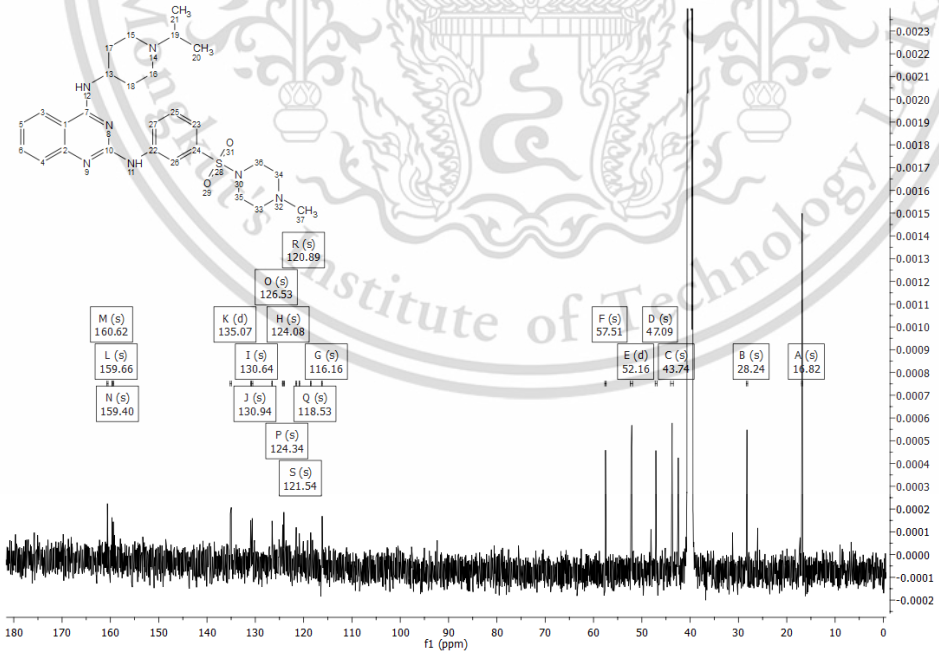

Figure 22. ^{13}C-NMR spectra of compound 25

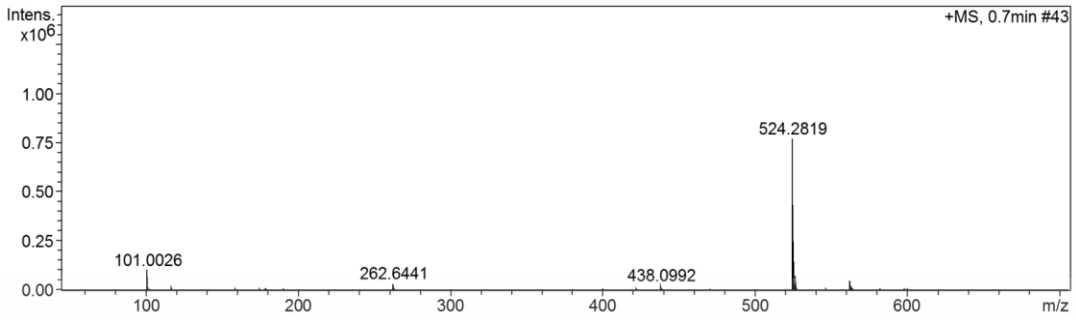

Figure 23. HRMS spectra of compound 25

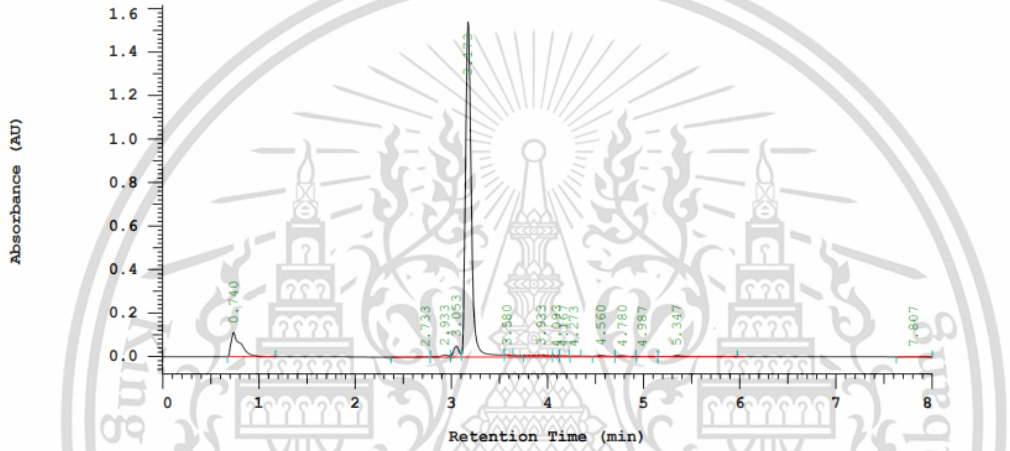

Figure 24. HPLC spectra of compound 25

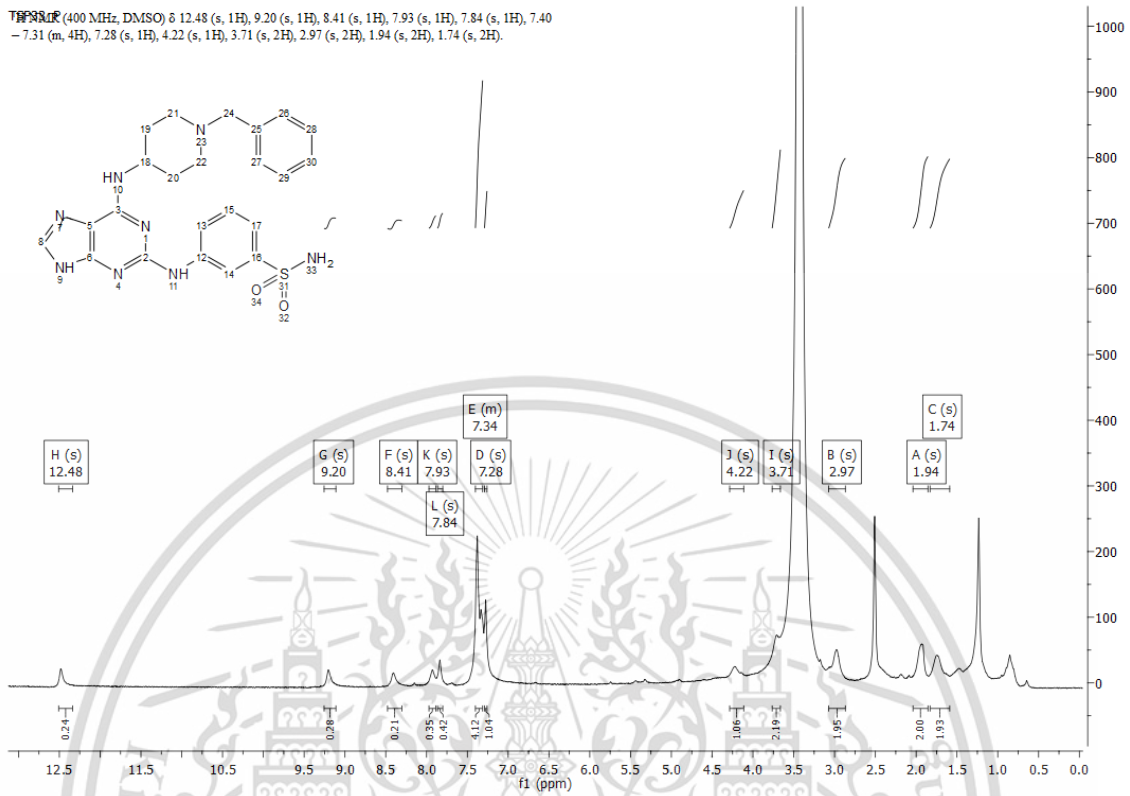

Figure 25. ^{1}H-NMR spectra of compound 36

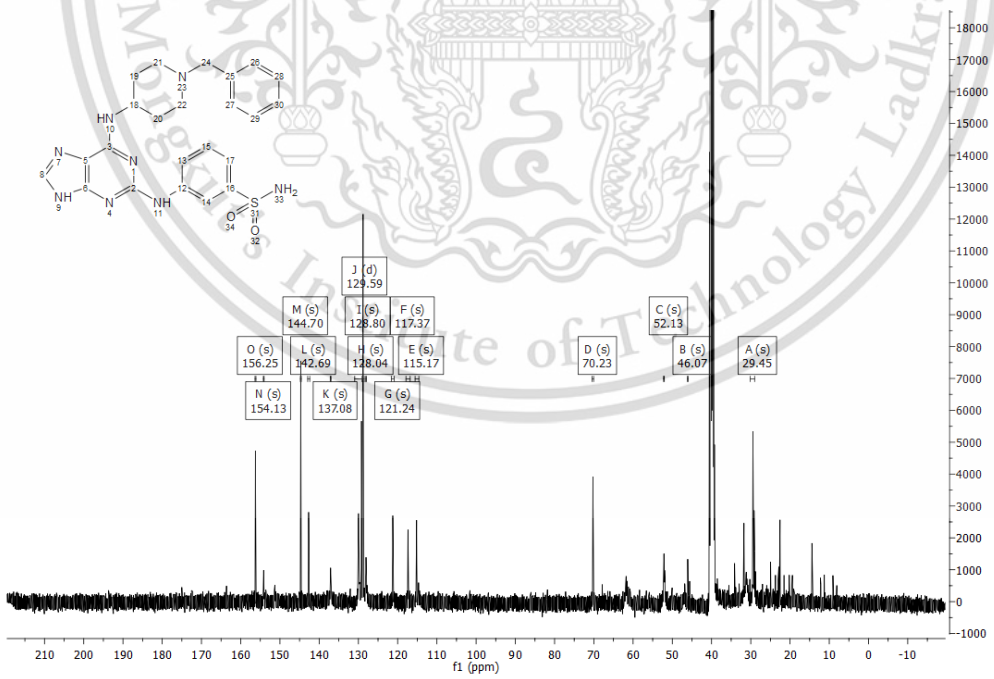

Figure 26. ^{13}C-NMR spectra of compound 36

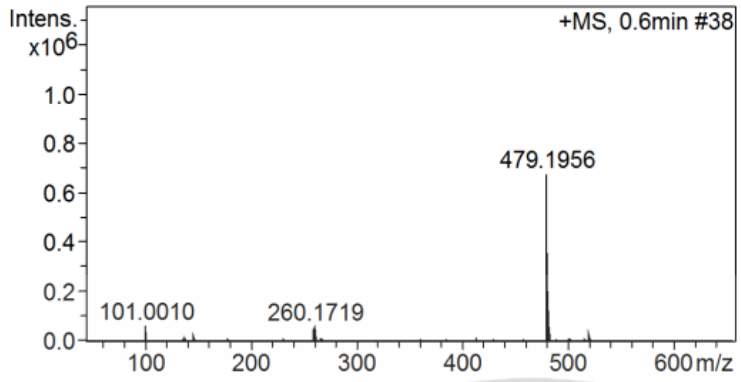

Figure 27. HRMS spectra of compound 36

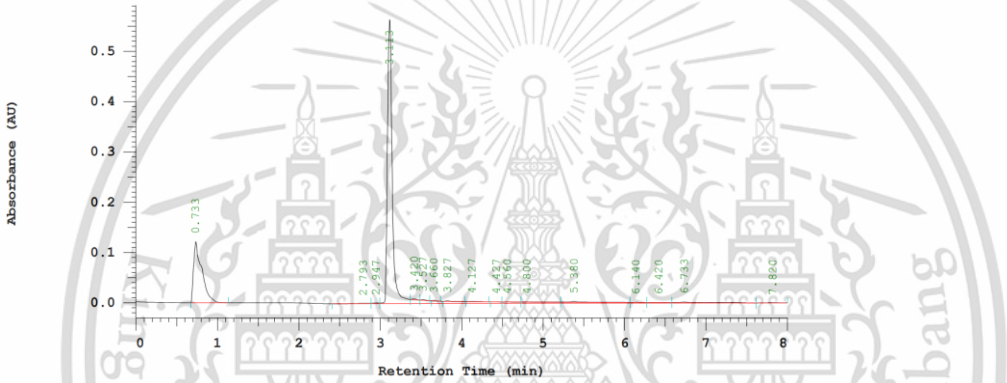

Figure 28. HPLC spectra of compound 36

4.6 PDE5 Inhibition

All compounds were evaluated for their activity against PDE5 at a concentration of 1 μM. %inhibition (%I) values ranged from 18 to 100% (Table 2). The IC_{50} of compounds that displayed a %I > 70% were subsequently determined. Observed IC_{50} ranged from 43 to 0.1 μM. Multiple compounds with sub μM potency were observed; **4**-**10**, **25**, **28** and **36**. Compounds **4** and **6** differ from the initial lead, **A**, by the introduction of a methylpiperazine group at the 3- and 4- position of aniline, respectively. Both compounds show approximately 5-fold higher IC_{50}s of 0.50 and 0.49 μM respectively. Compound **5,** substituted with the 3-SO_2-methylpiperazine substituent, has a comparable loss of activity at IC_{50} of 0.52 μM. This modification was introduced to reduce lipophilicity and solubility and is predicted to interact with solvent at the mouth of the active site, thus the subtle

drop in potency is not unsurprising (Figure 29). Compounds **7**-**10** replace the aromatic amine with propylamine and isopropylanime. These compounds were slightly more potent on average than **4**-**6**, with IC_{50}s ranging from 0.36-0.60 μM. Isopropylanime was marginally more potent than propyl amine. The subtly improved activity over aromatic substituents is consistent with the predicted binding mode given that Sildenafil employs a propyl group at the same location (Figure 8). Substitution of methylpiperazine at the meta- and para- positions of the anilino group did not appear to have a major effect on the PDE5 inhibitory activity. Compounds **11**-**13** retained the aliphatic groups at the 4-position of quinazoline in conjunction with methoxy substituents at the 6 and 7-positions. The compounds showed decreased in activity, with IC_{50} ranging from 1.44-3.97 μM. This appears to indicate the pocket cannot tolerate large groups, which is not unexpected given the predicted binding mode (Figure 29). Replacement of the quinazoline ring with 9-methyl-9H-purine was explored, leading to **14**-**21.** The derivatives contained both aliphatic (**16**-**19**) and aromatic amines (**14**,**15**,**20**-**21**). This structural alteration led to the least potent inhibitors overall, with IC_{50}s ranging from 4.46-43.16 μM. Analysis of the docking mode of exemplars to PDE5 suggested steric clash with residues, including Gln775. **23** was prepared, whereby, the 9-Me group was replaced with hydrogen. This resulted in a reduction in PDE5 IC_{50} to 2.02 μM. Analysis of the predicted binding mode suggests a potential H-bond interaction with the sidechain of Gln775. While, the compound was still considerably less potent than others reported here, the SAR appears to validate the predicted binding mode.

Compounds **24**-**28** introduced a basic moiety at 4-position of quinazoline. PDE5 IC_{50}s ranged from 0.15-9.39 μM. **25** was identified as the most potent of these, bearing an isopropyl piperidine at 4-position and methylpiperazine at 2-position. This dibasic compound had an IC_{50} of 0.15 μM, almost comparable to **A**, but with a considerably lower predicted lipophilicity ($JclogD_{7.4}$ of 3.9 vs 1.4). Additionally, **28** that was substituted by benzyl piperidine also displayed good activity, IC_{50} of 0.22 μM, but with slightly higher predicted $logD_{7.4}$ ($JclogD_{7.4}$ =2.65). The improved potency despite the general loss of lipophilicity, would be consistent with a binding mode whereby the basic center could interact with Asp764 (Figure 29). Finally, we also synthesized 6,7-dimethoxy quinazoline

with a basic moiety at 4-position. Compounds **29**, **30** and **34** had IC_{50} ranging from 1.64-3.41 μM confirming the general unsuitability of the OMe groups at this position, irrespective of what substituents are present at the 2- or 4-position of quinazoline. Two additional 9*H*-purine analogs were prepared with a basic group at the 6-position. **35** and **36** had IC_{50} of 0.29 μM and 32% inhibition at 1 μM, respectively. Comparing **36** to **23**, it appears that only one basic center is tolerated on the 9*H*-purine scaffold and that the 6-position is preferred.

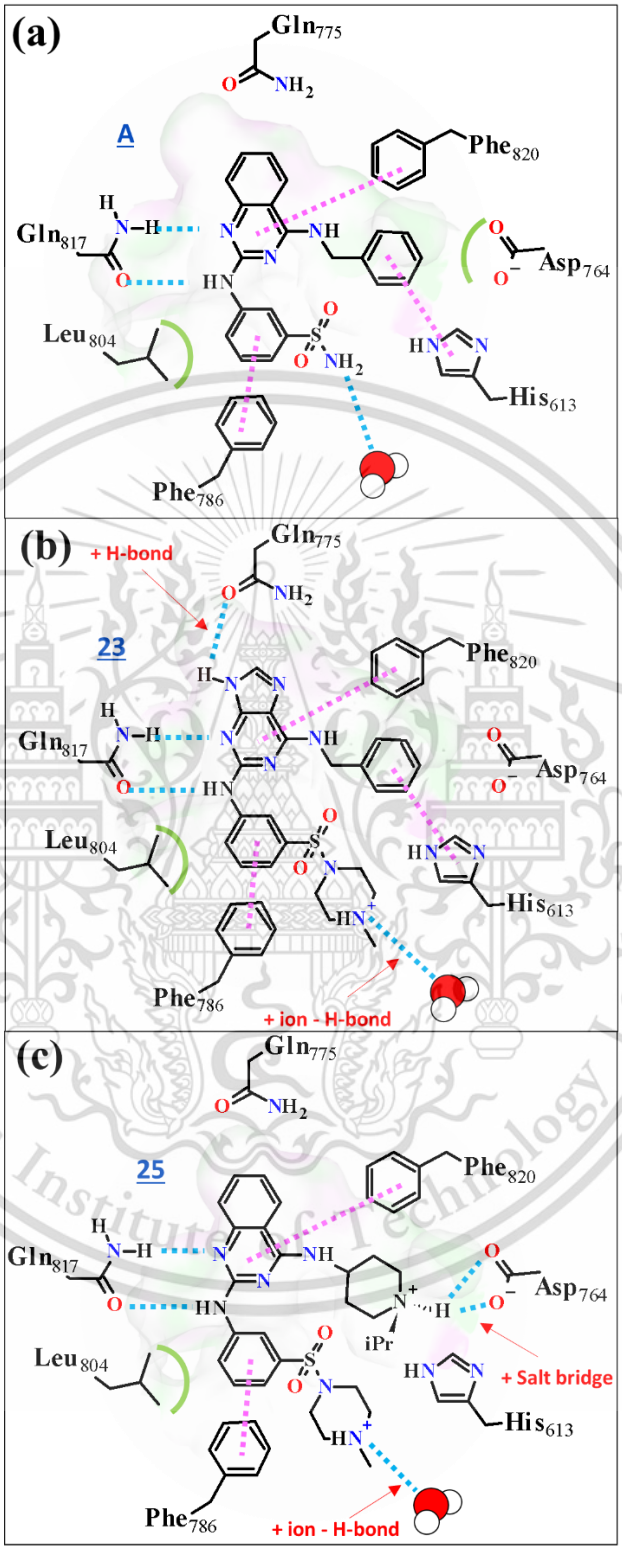

Figure 29. (a) 2D representation of (a) initial lead, **A**, (b) **23** and (c) **25** bound according to pose 2 in PDE5.

4.7 PDE1 Inhibition

The PDE5 inhibition data shows that multiple molecules with comparable potency to **A** were obtained, including **8**, **9**, **10**, **25**, **28**, **36**. These compounds display PDE5 activities approximately 100-fold lower than the standard Sildenafil. However, *ex vivo* studies comparing **A** to Sildenafil suggested such differences were not as pronounced.[15] Furthermore, It is known that PDE isoform selectivity is a leading cause of PDE5 inhibitor side effects.[69, 70] Sildenafil has a predicted PDE5/PDE1 selectivity ratio of 71-fold.[71] The 7 most active compounds were therefore evaluated in terms of their inhibition of the PDE1 isoform. Compounds were screened at 1 μM with IC_{50}s determined for compounds with %I >70%. Only compound, **A,** was found to inhibit PDE1 above the chosen threshold. The PDE1 IC_{50} was 11.83 μM, indicating ~100-folds selectivity over PDE5. This suggests compounds **25** and **36,** which have %I values of 28% and 31% respectively, will also demonstrate similar selectivity over PDE1.

Table 3. Partition coefficient ($logD_{7.4}$) and aqueous solubility and PDE1 activity of compounds **8**, **9**, **10**, **25**, **28**, **36** and sildenafil compared to **A**.

ID	$logD_{7.4}$	Sol. (mg/ mL)	%I PDE1[a]	IC_{50} PDE1 (μM)
Sildenafil	2.69	0.1790	nd	-
A	3.87	0.0021	73.87	11.83
8	3.92	0.0001	46.75	nd
9	3.55	0.0006	67.23	nd
10	3.68	0.0030	44.77	nd
25	2.15	1.7781	28.17	nd
28	3.37	0.0042	61.68	nd
36	2.16	0.1479	31.21	nd

4.8 Physico-chemical properties

A key goal in the further development of the chemotype was to improve the solubility as this can have a dramatic effect on more complex models. We therefore

determined the experimental solubility and lipophilicity for the Sildenafil**,** **A**, **8**, **9**, **10**, **25**, **28**, **36** using the shake flask technique (**Table 3**). Compounds **25** and **36** showed the lowest experimental $logD_{7.4}$ values (~2.1), lower than that of Sildenafil (2.7) and the initial lead compound **A** (3.87). Furthermore, compound **25** displayed approximately 10-fold improved solubility (1.8 mg/mL) compared to Sildenafil (0.18 mg/mL), and over 800 times greater than **A.** Only compounds **8** and **9**, where the 4-position benzyl was replaced by propyl and iso-propyl, respectively, had predicted solubilities lower than **A**.

Chapter 5

Conclusion

Twenty-nine new PDE5 inhibitors have been prepared based on our previously reported PDE5 lead **A**. Structure-based design was employed to aid in the development of structural modification of the series. We determined the binding mode of **A** to PDE5 using a protocol involving QM ligand optimization, ligand-based overlap to known active conformations, and a combined molecular docking and MD protocol to identify the putative binding mode of compounds. This consensus approach led to the identification of a single binding mode that was consistent with (a) the experimental binding modes of PDE5 inhibitors, and (b) with the experimental SAR generated in the study. Seven compounds demonstrated equivalent inhibitory activity to PDE5 compared to **A**. Compound **25** was found to have the best combination of PDE5 activity (IC_{50} at 0.15 μM), selectivity over the PDE1 isoform (%I at μM of 28%) and low experimental $logD_{7.4}$ (2.15). The compound also displayed good solubility (1.8 mg/mL), which was 10-fold greater than Sildenafil and 800-fold better than **A** itself.

In summary, we have validated a computationally driven strategy to design new derivatives of **A** with equivalent activity, improved solubility and PDE1 selectivity. This work highlights the value of molecular modelling in structure-based design and will influence the next iteration of derivatives that will focus on improving the PDE5 activity.

Reference

1. Barret, R., *1 - Medicines and Drugs*, in *Therapeutical Chemistry*, R. Barret, Editor. 2018, Elsevier. p. 1-20.
2. Humbert, M., et al., *Pulmonary arterial hypertension in France: results from a national registry.* Am J Respir Crit Care Med, 2006. **173**(9): p. 1023-30.
3. Wilkins, M., et al., *Recent advances in pulmonary arterial hypertension [version 1; peer review: 2 approved].* F1000Research, 2018. **7**(1128).
4. Beshay, S., S. Sahay, and M. Humbert, *Evaluation and management of pulmonary arterial hypertension.* Respiratory Medicine, 2020. **171**.
5. Lim, Y., et al., *Pulmonary arterial hypertension in a multi-ethnic Asian population: Characteristics, survival and mortality predictors from a 14-year follow-up study.* Respirology, 2019. **24**(2): p. 162-170.
6. Raja, S.G., et al., *Treatment of pulmonary arterial hypertension with sildenafil: from pathophysiology to clinical evidence.* J Cardiothorac Vasc Anesth, 2006. **20**(5): p. 722-35.
7. Roldan, T., et al., *Safety and tolerability of targeted therapies for pulmonary hypertension in children.* Pediatr Cardiol, 2014. **35**(3): p. 490-8.
8. Gaffuri, M., et al., *Acute onset of bilateral visual loss during sildenafil therapy in a young infant with congenital heart disease.* BMJ Case Rep, 2014. **2014**.
9. Lüke, M., et al., *Effects of phosphodiesterase type 5 inhibitor sildenafil on retinal function in isolated superfused retina.* J Ocul Pharmacol Ther, 2005. **21**(4): p. 305-14.
10. Berman, H.M., et al., *The Protein Data Bank.* Nucleic Acids Research, 2000. **28**(1): p. 235-242.
11. Takase, Y., et al., *Cyclic GMP Phosphodiesterase Inhibitors. 2. Requirement of 6-Substitution of Quinazoline Derivatives for Potent and Selective Inhibitory Activity.* Journal of Medicinal Chemistry, 1994. **37**(13): p. 2106-2111.
12. Lee, S.J., et al., *Discovery of potent cyclic GMP phosphodiesterase inhibitors. 2-Pyridyl- and 2-imidazolylquinazolines possessing cyclic GMP phosphodiesterase*

and thromboxane synthesis inhibitory activities. J Med Chem, 1995. **38**(18): p. 3547-57.

13. Pobsuk, N., et al., *Design, synthesis and evaluation of N-2,N-4-diaminoquinazoline based inhibitors of phosphodiesterase type 5.* Bioorganic & Medicinal Chemistry Letters, 2019. **29**(2): p. 267-270.
14. Hughes, R.O., et al., *Investigation of the pyrazinones as PDE5 inhibitors: Evaluation of regioisomeric projections into the solvent region.* Bioorganic & Medicinal Chemistry Letters, 2011. **21**(21): p. 6348-6352.
15. Paracha, T., et al., *Elucidation of Vasodilation Response and Structure Activity Relationships of N2,N4-Disubstituted Quinazoline 2,4-Diamines in a Rat Pulmonary Artery Model.* Molecules, 2019. **24**: p. 281.
16. Dhariwal, A.K. and S.B. Bavdekar, *Sildenafil in pediatric pulmonary arterial hypertension.* J Postgrad Med, 2015. **61**(3): p. 181-92.
17. Simonneau, G., et al., *Updated clinical classification of pulmonary hypertension.* J Am Coll Cardiol, 2013. **62**(25 Suppl): p. D34-41.
18. Tuder, R.M., et al., *Relevant issues in the pathology and pathobiology of pulmonary hypertension.* J Am Coll Cardiol, 2013. **62**(25 Suppl): p. D4-12.
19. Hatton, N. and J.J. Ryan, *Sex differences in response to pulmonary arterial hypertension therapy: is what's good for the goose, good for the gander?* Chest, 2014. **145**(6): p. 1184-1186.
20. Ling, Y., et al., *Changing demographics, epidemiology, and survival of incident pulmonary arterial hypertension: results from the pulmonary hypertension registry of the United Kingdom and Ireland.* Am J Respir Crit Care Med, 2012. **186**(8): p. 790-6.
21. Coons, J.C., et al., *Pulmonary Arterial Hypertension: a Pharmacotherapeutic Update.* Curr Cardiol Rep, 2019. **21**(11): p. 141.
22. Parikh, V., A. Bhardwaj, and A. Nair, *Pharmacotherapy for pulmonary arterial hypertension.* J Thorac Dis, 2019. **11**(Suppl 14): p. S1767-s1781.
23. Rivera-Lebron, B.N. and M.G. Risbano, *Ambrisentan: a review of its use in pulmonary arterial hypertension.* Ther Adv Respir Dis, 2017. **11**(6): p. 233-244.

24. Humbert, M. and H.A. Ghofrani, *The molecular targets of approved treatments for pulmonary arterial hypertension.* Thorax, 2016. **71**(1): p. 73-83.

25. Klinger, J.R. and P.J. Kadowitz, *The Nitric Oxide Pathway in Pulmonary Vascular Disease.* Am J Cardiol, 2017. **120**(8s): p. S71-s79.

26. DeNinno, M.P., *Future directions in phosphodiesterase drug discovery.* Bioorganic & Medicinal Chemistry Letters, 2012. **22**(22): p. 6794-6800.

27. Mehats, C., et al., *Cyclic nucleotide phosphodiesterases and their role in endocrine cell signaling.* Trends in Endocrinology & Metabolism, 2002. **13**(1): p. 29-35.

28. Biswas, K.H., S. Sopory, and S.S. Visweswariah, *The GAF Domain of the cGMP-Binding, cGMP-Specific Phosphodiesterase (PDE5) Is a Sensor and a Sink for cGMP.* Biochemistry, 2008. **47**(11): p. 3534-3543.

29. Corbin, J.D., *Mechanisms of action of PDE5 inhibition in erectile dysfunction.* Int J Impot Res, 2004. **16 Suppl 1**: p. S4-7.

30. Ahmed, W.S., A.M. Geethakumari, and K.H. Biswas, *Phosphodiesterase 5 (PDE5): Structure-function regulation and therapeutic applications of inhibitors.* Biomedicine & Pharmacotherapy, 2021. **134**: p. 111128.

31. Barker, A.J., et al., *Studies leading to the identification of ZD1839 (IRESSA): an orally active, selective epidermal growth factor receptor tyrosine kinase inhibitor targeted to the treatment of cancer.* (0960-894X (Print)).

32. Wu, X., et al., *Design and synthesis of novel Gefitinib analogues with improved anti-tumor activity.* (1464-3391 (Electronic)).

33. Van Horn, K.S., et al., *Antileishmanial activity of a series of N²,N⁴-disubstituted quinazoline-2,4-diamines.* Journal of medicinal chemistry, 2014. **57**(12): p. 5141-5156.

34. Sharma, S., et al., *Design strategies, structure activity relationship and mechanistic insights for purines as kinase inhibitors.* (1768-3254 (Electronic)).

35. Hei, Y.Y., et al., *Synthesis and evaluation of 2,9-disubstituted 8-phenylthio/phenylsulfinyl-9H-purine as new EGFR inhibitors.* (1464-3391 (Electronic)).

36. Abraham, R.T., et al., *Cellular effects of olomoucine, an inhibitor of cyclin-dependent kinases.* (0248-4900 (Print)).

37. Lamanna, N. and M. Weiss, *Purine analogs in leukemia.* (1054-3589 (Print)).

38. Craig, S.P., 3rd and A.E. Eakin, *Structure-based inhibitor design.* Vitam Horm, 2000. **58**: p. 149-69.

39. Wang, G., et al., *Design, Synthesis, and Pharmacological Evaluation of Monocyclic Pyrimidinones as Novel Inhibitors of PDE5.* Journal of Medicinal Chemistry, 2012. **55**(23): p. 10540-10550.

40. Pobsuk, N., et al., *Design, synthesis and evaluation of N(2),N(4)-diaminoquinazoline based inhibitors of phosphodiesterase type 5.* Bioorg Med Chem Lett, 2019. **29**(2): p. 267-270.

41. Frisch, M.J., et al., *Gaussian 16 Rev. C.01*. 2016: Wallingford, CT.

42. Card, G.L., et al., *Structural Basis for the Activity of Drugs that Inhibit Phosphodiesterases.* Structure, 2004. **12**(12): p. 2233-2247.

43. Sung, B.-J., et al., *Structure of the catalytic domain of human phosphodiesterase 5 with bound drug molecules.* Nature, 2003. **425**(6953): p. 98-102.

44. Hsieh, C.-M., et al., *Structure of Human Phosphodiesterase 5A1 Complexed with Avanafil Reveals Molecular Basis of Isoform Selectivity and Guidelines for Targeting α-Helix Backbone Oxygen by Halogen Bonding.* Journal of Medicinal Chemistry, 2020. **63**(15): p. 8485-8494.

45. Vainio, M.J., J.S. Puranen, and M.S. Johnson, *ShaEP: Molecular Overlay Based on Shape and Electrostatic Potential.* Journal of Chemical Information and Modeling, 2009. **49**(2): p. 492-502.

46. Schneidman-Duhovny, D., et al., *PharmaGist: a webserver for ligand-based pharmacophore detection.* Nucleic Acids Research, 2008. **36**(suppl_2): p. W223-W228.

47. Schneidman-Duhovny, D., et al., *Deterministic pharmacophore detection via multiple flexible alignment of drug-like molecules.* J Comput Biol, 2008. **15**(7): p. 737-54.

48. *GOLD5.3:* https://www.ccdc.cam.ac.uk/solutions/csd-discovery/components/gold/.

49. Abraham, M.J., et al., *GROMACS: High performance molecular simulations through multi-level parallelism from laptops to supercomputers.* SoftwareX, 2015. **1-2**: p. 19-25.

50. Hornak, V., et al., *Comparison of multiple Amber force fields and development of improved protein backbone parameters.* Proteins: Struct., Funct., Bioinf., 2006. **65**(3): p. 712-725.

51. Thompson, E., et al., *Evaluating Molecular Mechanical Potentials for Helical Peptides and Proteins.* PLoS ONE, 2010. **5**(4): p. e10056.

52. Sousa da Silva, A.W. and W.F. Vranken, *ACPYPE - AnteChamber PYthon Parser interfacE.* BMC Res.Notes, 2012(5): p. 367.

53. Wang, J., et al., *Automatic Atom Type And Bond Type Perception In Molecular Mechanical Calculations.* J. Mol. Graph. Model., 2006. **25**(2): p. 247-260.

54. Wang, J., et al., *Development and testing of a general amber force field.* Journal of Computational Chemistry, 2004. **25**(9): p. 1157-1174.

55. Olsson, M.H.M., et al., *PROPKA3: Consistent Treatment of Internal and Surface Residues in Empirical pKa Predictions.* Journal of Chemical Theory and Computation, 2011. **7**(2): p. 525-537.

56. Søndergaard, C.R., et al., *Improved Treatment of Ligands and Coupling Effects in Empirical Calculation and Rationalization of pKa Values.* Journal of Chemical Theory and Computation, 2011. **7**(7): p. 2284-2295.

57. Price, D.J. and C.L. Brooks, *A modified TIP3P water potential for simulation with Ewald summation.* The Journal of Chemical Physics, 2004. **121**(20): p. 10096-10103.

58. Parrinello, M. and A. Rahman, *Polymorphic transitions in single crystals: A new molecular dynamics method.* Journal of Applied Physics, 1981. **52**(12): p. 7182-7190.

59. Van Der Spoel, D., et al., *GROMACS: Fast, flexible, and free.* Journal of Computational Chemistry, 2005. **26**(16): p. 1701-1718.

60. Hess, B., et al., *LINCS: A Linear Constraint Solver for Molecular Simulations.* J. Comput. Chem., 1997. **18**: p. 1463-1472.

61. Srivilai, J., et al., *Phenanthrene-enriched extract from Eulophia macrobulbon using subcritical dimethyl ether for phosphodiesterase-5A1 inhibition.* Scientific Reports, 2022. **12**(1): p. 5992.

62. Bhandari, S., et al., *At-line LC-QTOF-MS micro-fractionation of Derris scandens (Roxb.) Benth, coupled to radioassay for the early identification of PDE5A1 inhibitors.* Phytochemical Analysis, 2020. **31**(3): p. 297-305.

63. Wenlock, M.C., et al., *A Highly Automated Assay for Determining the Aqueous Equilibrium Solubility of Drug Discovery Compounds.* J. Assoc. Lab. Auto., 2011. **16**(4): p. 276-284.

64. Wenlock, M.C., et al., *A Method for Measuring the Lipophilicity of Compounds in Mixtures of 10.* Journal of Biomolecular Screening, 2011. **16**(3): p. 348-355.

65. Boström, J., A. Hogner, and S. Schmitt, *Do Structurally Similar Ligands Bind in a Similar Fashion?* Journal of Medicinal Chemistry, 2006. **49**(23): p. 6716-6725.

66. Warren, G.L., et al., *A critical assessment of docking programs and scoring functions.* J Med Chem, 2006. **49**(20): p. 5912-31.

67. Berendsen, H.J.C., et al., *Molecular Dynamics with Coupling to an External Bath.* J. Chem. Phys., 1984. **81**(8): p. 3684-3690.

68. Vijay Kumar, D., et al., *Lead optimization of purine based orally bioavailable Mps1 (TTK) inhibitors.* Bioorg Med Chem Lett, 2012. **22**(13): p. 4377-85.

69. Laties, A.M. and E. Zrenner, *Viagra® (sildenafil citrate) and ophthalmology.* Progress in Retinal and Eye Research, 2002. **21**(5): p. 485-506.

70. Huang, S.A. and J.D. Lie, *Phosphodiesterase-5 (PDE5) Inhibitors In the Management of Erectile Dysfunction.* P & T : a peer-reviewed journal for formulary management, 2013. **38**(7): p. 407-419.

71. Wallis, R.M., *The pharmacology of sildenafil, a novel and selective inhibitor of phosphodiesterase (PDE) type 5.* Nihon Yakurigaku Zasshi, 1999. **114 Suppl 1**: p. 22p-26p.